

Set2Seq Transformer: Temporal and Positional-Aware Set Representations for Sequential Multiple-Instance Learning

Athanasios Efthymiou^{*}, Stevan Rudinac, Monika Kackovic, Nachoem Wijnberg[†], Marcel Worring

University of Amsterdam

Amsterdam, The Netherlands

{a.efthymiou,s.rudinac,m.kackovic,n.m.wijnberg,m.worring}@uva.nl

Abstract

Sequential multiple-instance learning involves learning representations of sets distributed across discrete timesteps. In many real-world applications, modeling both the internal structure of sets and their temporal relationships across time is essential for capturing complex underlying patterns. However, existing methods either focus on learning set representations at a static level, ignoring temporal dynamics, or treat sequences as ordered lists of individual elements, lacking explicit mechanisms to represent sets. In this work, we propose Set2Seq Transformer, a novel architecture that jointly models permutation-invariant set structure and temporal dependencies by learning temporal and positional-aware representations of sets within a sequence in an end-to-end multimodal manner. We evaluate our Set2Seq Transformer on two tasks that require modeling both set structure alongside temporal and positional patterns, but differ significantly in domain, modality, and objective. First, we consider a fine-art analysis task, modeling artists’ oeuvres for predicting artistic success using a novel dataset, WikiArt-Seq2Rank. Second, we utilize our Set2Seq Transformer for a short-term wildfire danger forecasting task. Through extensive experimentation, we show that our Set2Seq Transformer significantly improves over traditional static multiple-instance learning methods by effectively learning permutation-invariant set, temporal, and positional-aware representations across diverse domains, modalities, and tasks. We will release both the dataset and model implementations on GitHub.

CCS Concepts

• **Computing methodologies** → Image representations; **Instance-based learning**; • **Information systems** → Learning to rank; • **Applied computing** → Arts and humanities.

Keywords

multiple-instance learning, sequence modeling, visual learning-to-rank, fine-art analysis, wildfire modeling

1 Introduction

Learning representations of sequences of sets is essential in various domains, such as in detecting transients in observational cosmology [1, 37, 90, 115], predicting microsatellite status in biomedical and public health tasks [3, 62], analyzing cultural phenomena [44, 130], or environmental forecasting [66, 104]. The advances in deep learning have inspired work in various real-world tasks in multimedia and related disciplines that require learning representations of set-structured inputs, ranging from 3D point cloud classification [22,

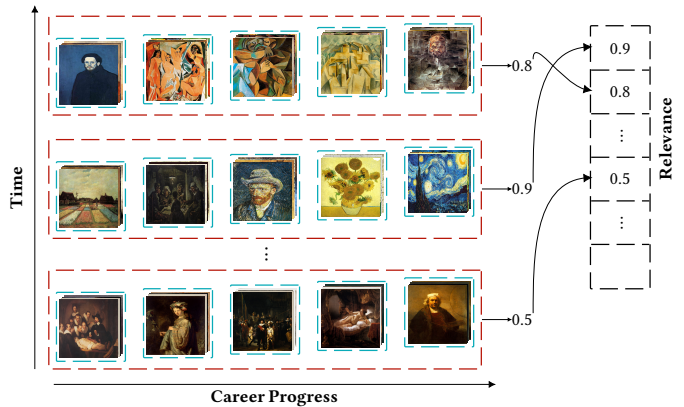


Figure 1: Illustration of sequential multiple-instance learning for predicting artists’ success with respect to a specific criterion. Given an artist’s body of work as a sequence (depicted in red) of sets of artworks (depicted in cyan) created at discrete timesteps, the task is to predict the artist’s success according to the criterion. The horizontal axis represents the artist’s career stage, while the vertical axis the temporal aspect. We utilize positional encodings to represent the relative order of discrete timesteps within an artist’s career, with learnable embeddings for the absolute time values (e.g., year) associated with each timestep.

51, 95, 119, 131] and anomaly detection [70, 138, 139] to few-shot learning [67, 71, 106, 120] and beyond [42, 56, 97, 119], primarily in static settings. Sequential multiple-instance scenarios arise naturally in diverse real-world applications, such as environmental forecasting—where each timestep contains spatially distributed sensor readings relevant for wildfire prediction [66, 104]—or analyzing visual artists’ oeuvres, where each timestep corresponds to a set of artworks produced within a particular period of an artist’s career [76, 77, 102].

Unlike standard supervised learning scenarios where inputs are individual elements with fixed ordering, sequential multiple-instance learning considers inputs in which each timestep comprises an unordered set of instances. Set-based representation methods [56, 70, 105, 138, 139] can effectively model permutation-invariant relationships within individual sets, but operate almost exclusively at a static level, assuming no interactions among sets over time. Conversely, sequential modeling methods [15, 33, 118] are effective at capturing long-range temporal dependencies in ordered data, but process inputs as sequences of individual elements, lacking explicit mechanisms to represent sets. Existing methods thus fail to jointly learn

^{*}Corresponding author.

[†]Also affiliated with University of Johannesburg.

permutation-invariant representations of individual sets and model the temporal dependencies among them.

In this work, we propose Set2Seq Transformer for end-to-end sequential multiple-instance learning. Our Set2Seq Transformer integrates multiple-instance learning and sequential modeling to jointly learn set and sequence representations, modeling two distinct yet complementary types of structure—temporal and positional-aware representations. We argue that encoding position-aware representations of observed events in a fixed and finite time interval, for instance physical occurrences at a known and predefined point, such as a calendar season, can capture local phenomena occurring in this finite space. In addition, learning temporal representations of observed events in discrete timesteps across not predefined and almost infinite time intervals, such as calendar years, can capture global characteristics of the interaction among different phenomena. For instance, as shown in Figure 1, modeling visual artists’ oeuvres requires reasoning over sets of artworks created at discrete timesteps, where both the relative stage within an artist’s career and the absolute year offer complementary temporal signals essential for predicting long-term artistic success. Integrating set, temporal, and position-aware representations enables learning permutation-invariant representations of sets while capturing both local and global temporal structure across sequences of sets.

We evaluate the performance of our Set2Seq Transformer, focusing on two distinct tasks, namely predicting artistic success and short-term wildfire danger forecasting. For the task of predicting artistic success, we introduce a novel dataset, WikiArt-Seq2Rank, which consists of 58,458 artworks created by 849 renowned artists, as well as rankings of artistic performance using multiple representative indicators. For the wildfire forecasting task, we use the publicly available Mesogeos dataset [66], which involves predicting short-term wildfire danger from spatially distributed environmental observations evolving over time. These two diverse tasks enable a systematic evaluation of the performance of our Set2Seq Transformer in modeling permutation-invariant set structure alongside temporal and positional information across distinct domains. In summary, our main contributions are as follows:

- We introduce the Set2Seq Transformer, a novel architecture that jointly learns permutation-invariant set, temporal, and positional-aware representations for end-to-end sequential multiple-instance learning.
- We introduce the WikiArt-Seq2Rank dataset and the associated visual learning-to-rank task for predicting artistic performance across multiple representative success indicators, and evaluate our Set2Seq Transformer against several static and sequential multiple-instance learning methods.
- We further evaluate our Set2Seq Transformer on the Mesogeos dataset for short-term wildfire danger forecasting.
- We extend the short-term wildfire danger forecasting task by introducing a proactive early forecasting setup, assessing performance under gradually increasing temporal context.
- We comprehensively benchmark our Set2Seq Transformer, demonstrating its effectiveness and generalizability across structurally and semantically distinct tasks.

The remainder of this paper is structured as follows. In Section 2, we review relevant literature on multiple-instance learning, learning

position-aware representations, visual learning-to-rank and learning visual representations for fine-art analysis. In Section 3, we provide the details of our Set2Seq Transformer architecture and, thereafter, in Section 4 we present the experimental setup. Finally, in Section 5 we report the experimental results, and in Section 6 we conclude with a brief summary of our findings.

2 Related Work

Advancements in deep learning have inspired research in both static and sequential multiple-instance learning [70, 119, 138, 139]. Furthermore, the remarkable achievements in modern computer vision and multimedia have spurred research in diverse applications, such as visual learning-to-rank tasks [23, 93, 117, 122] and automated fine-art analysis [39, 40, 45, 107]. In this section, we briefly survey representative methods developed within each of these research domains.

2.1 Multiple-Instance Learning

Multiple-instance learning has been a subject of extensive and long-standing research [35, 84]. Several works have recently achieved remarkable performance on various multiple-instance learning tasks. PointNet [22], DeepSets [138], and RepSet [105] focus on permutation-invariant and equivariant set representations, leveraging aggregation operators and matching flow techniques. Ilse et al. [56] utilize attention-based modules to provide a better insight into the contribution of each label within sets. Lee et al. [70] propose Set Transformer, a Transformer-based architecture that employs self-attention for modeling permutation-invariant representations. Zhang et al. [139] address some of the limitations of DeepSets [138] and Set Transformer [70] architectures achieving better or comparable performance on different benchmarks.

Recently, the deep learning advancements have inspired research in sequential multiple-instance learning [12, 59, 60, 78]. The seminal work of Vinyals et al. [119] utilizes the seq2seq framework to learn the order of sets by employing Recurrent Neural Networks (RNNs), and more specifically Long Short Term Memory network (LSTMs) [53], coupled with attention-mechanism. Several works extend this approach for various tasks, such as sentence ordering [11, 68, 81, 123], text summarization [108] and multi-agent systems [109]. In contrast to previous work, we utilize DeepSets and Set Transformer, which are traditionally used for static set representation, to learn representations of sets in a sequential manner. Our proposed approach not only preserves the permutation invariance within each set but also captures the relative positions of sets across sequences, integrating both positional and temporal information.

2.2 Learning Temporal-Aware Representations

Sequence modeling is a long-standing research topic [7, 26, 46, 49, 53, 61, 110, 124]. Intrinsically modeling sequences using Recurrent Neural Networks (RNNs) [99] and several of its variants [26, 53] has been successfully applied in many different tasks and settings [61, 110, 119]. Even though, learning explicit position-aware representations [46] has been also successfully applied, the tremendous success of transformers [118] has paved the way to learning representations of time by utilizing various position-aware methods.

Our work is closely related to [119] which argues that learning intrinsic representations of sequential order is essential for a variety

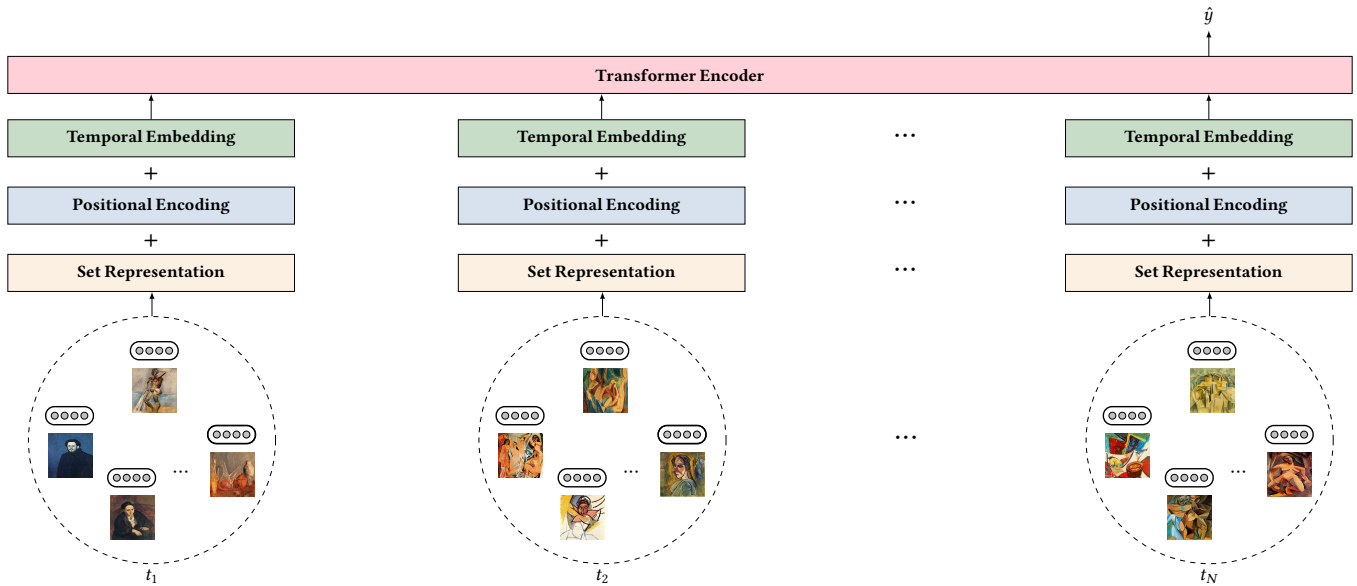


Figure 2: This figure illustrates the Set2Seq Transformer. For an ordered sequence \mathcal{T} of unordered sets \mathcal{S} , we learn a representation s_i for each set at timestep t_i . Positional encoding u_i and temporal embedding v_i are used for each timestep t_i , and summed with s_i to obtain the final representation τ_i for the timestep t_i . These representations are then passed through a Transformer encoder, followed by a fully-connected layer, to generate the final prediction \hat{y} , derived from the last timestep t_N .

of tasks. Inspired by successes of learning position-aware representations [33, 46, 118], we utilize position-aware representations for different timesteps. However, unlike prior work, our approach uses two distinct mechanisms: one for encoding the relative position of sets within sequences and another for learning temporal embeddings that capture progression over time.

2.3 Visual Learning-to-Rank

Learning-to-rank is one of the most prominent tasks in information retrieval and it has been successfully applied in a number of works [11, 81, 123]. Recent advancements in computer vision and the large amount of available datasets has increased research also in visual learning-to-rank. For instance, van den Akker et al. [117] proposes ViTOR, a method that learns to rank webpages solely based on their visual appearance. In addition, many visual learning-to-rank approaches have been adapted for the specific application of age estimation [23, 75, 93]. Contrary to this line of research, which typically focus on ranking individual images or instances based on estimated age, our approach is a point-wise visual learning-to-rank method that ranks entire sequences of sets, capturing both temporal dependencies and relative positioning across multiple sets within a sequence.

2.4 Automatic Fine-Art Analysis

The large amount of publicly available art-related datasets [107, 111, 128, 137] has inspired research in learning visual representations for various fine-art analysis tasks, ranging from fine-art categorization [18, 39, 40, 45] and studying semantic principles of the fine-art history [19, 20, 65] to style transfer [32, 55, 132] among many others [8, 9, 13, 21, 83, 89]. In contrast to these works, we do not rely

solely on learning representations of artworks at a static single-instance level, but we learn representations of sequences of sets of artworks created by distinct artists to predict artistic performance across multiple representative success indicators.

3 Set2Seq Transformer

We now present Set2Seq Transformer, a novel framework for learning temporal and positional-aware representations of sequences of sets in sequential multiple-instance learning. Each sequence consists of ordered sets, where each set contains multiple instances, and the task is to compute a target value associated with the sequence. To this end, the Set2Seq Transformer first learns permutation-invariant representations of individual sets and then encodes the sequence by leveraging two distinct mechanisms: one for encoding the relative positions of sets within the sequence and another for capturing temporal dynamics through learnable embeddings over time. These enriched representations are processed by a Transformer encoder, adaptable to diverse objectives, such as learning-to-rank or classification. Figure 2 depicts our proposed Set2Seq Transformer architecture.

3.1 Set Representation Learning

As the learned representation should not change for any permutation of the instances within the set, permutation-invariant representations of set-structured inputs are essential. Several methods have recently been proposed to learn permutation-invariant representations of sets [56, 70, 138, 139]. Here, we focus on learning permutation-invariant representations of sets of multiple visual instances.

Learning permutation-invariant set representations. Let \mathcal{S} denote an unordered set of instances, such as:

$$\mathcal{S} = \{x_1, x_2, \dots, x_n\}, \quad (1)$$

where x_i denotes the i^{th} instance in the set \mathcal{S} and n the total number of instances within the set \mathcal{S} . Our task is to learn a permutation-invariant representation \mathbf{s} for the set \mathcal{S} so that \mathbf{s} does not change under any permutation of the instances within \mathcal{S} . For our Set2Seq Transformer, we utilize the DeepSets [138] and Set Transformer [70] architectures as two set-based alternative methods for learning set representations of \mathcal{S} . For both methods, we use a final fully-connected layer to obtain an H -dimensional set representation $\mathbf{s} \in \mathbb{R}^H$. We considered utilizing the DeepSets++ and Set Transformer++ as provided in [139], but we did not observe any significant improvement using deeper architectures and normalization layers for our specific tasks.

DeepSets. For DeepSets, we use four fully-connected layers as the encoder followed by the aggregation operation and a decoder of three fully-connected layers. The dimensionality of all hidden layers is set to $H/2$, i.e., 256. We consider two pooling operations, average (mean) and maximum (max) pooling, and employ the Rectified Linear Unit (ReLU) activation between layers in both encoder and decoder.

Set Transformer. For Set Transformer, we consider three different variants. First, we use a Set Transformer with stacked Set Attention Blocks (SAB) followed by a Pooling by Multi-head Attention (PMA) module, which we refer to as Set Transformer (SAB + PMA). We also consider a Set Transformer with stacked Induced Set Attention Blocks (ISAB) followed by PMA, Set Transformer (ISAB + PMA). Finally, we consider a Set Transformer with stacked ISAB blocks followed by PMA and stacked SAB modules, Set Transformer (ISAB + PMA + SAB). We again set the dimensionality of all hidden layers to $H/2$, i.e., 256, and the number of attention heads to 4.

Visual instance representation. To extract feature vectors to represent a visual instance x_i , we utilize a backbone pre-trained on ImageNet [31] and frozen ResNet-34 [52]. Following the same notation as in [39], for a given visual instance x_i , we can obtain a visual representation \mathbf{x}_i as follows:

$$\mathbf{x}_i = F_{GAP}(f_{ResNet-34}(\mathcal{P}; \theta_{ResNet-34})) \in \mathbb{R}^H, \quad (2)$$

where \mathcal{P} denotes the artwork’s photographic reproduction, F_{GAP} denotes the global average pooling operation, $\theta_{ResNet-34}$ denotes the ResNet-34 parameters, and H denotes the dimensionality of the resulting visual embedding, i.e., 512.

Numerical instance representation. The Mesogeos dataset, used for short-term wildfire danger forecasting, encompasses 24 variables related to known fire drivers, including meteorology, vegetation, land cover, and human activity, with features derived from both satellite observations (e.g., vegetation indices) and ground measurements (e.g., temperature, humidity). For each numerical instance x_i , we normalize these features and encode \mathbf{x}_i through a fully connected layer, yielding an embedding of size $H = 512$.

3.2 Sequential Learning

Inspired by its remarkable success, we use the Transformer [118] architecture to learn sequential representations. Following [33, 118], we utilize temporal-aware representations and a Transformer encoder module.

Learning representation of sequences. We learn permutation-invariant representations of the sets \mathcal{S} observed at different timesteps t . Let \mathcal{T} denote the sequence of such sets:

$$\mathcal{T} = \{\mathcal{S}_1, \mathcal{S}_2, \dots, \mathcal{S}_N\}, \quad (3)$$

where each \mathcal{S}_i is the set of instances observed at timestep t_i . Our task is to learn a permutation-invariant representation of $\mathcal{T} \in \mathbb{R}^{N \times H}$ to predict the target value for \mathcal{T} .

Positional encoding. Following [118], we use positional encodings $\mathbf{u}_i \in \mathbb{R}^H$ for encoding the relative position of a timestep t_i within \mathcal{T} . We use sine and cosine functions to capture relative positions through smooth periodic patterns that generalize to unseen sequence lengths. We obtain \mathbf{u}_i at t_i as follows:

$$\mathbf{u}_i(t_i, 2l) = \sin(t/k^{2l/H}), \quad (4)$$

$$\mathbf{u}_i(t_i, 2l+1) = \cos(t/k^{2l/H}), \quad (5)$$

where t_i denotes the position of i^{th} timestep in the input sequence \mathcal{T} , and l the l^{th} dimension index of the H -dimensional embedding.

Temporal embedding. Inspired by [33, 46, 118, 133], in addition to the positional encoding \mathbf{u}_i , we learn independent temporal-aware embeddings $\mathbf{v}_i \in \mathbb{R}^H$ that correspond to the temporal value associated with a given timestep t_i , e.g., the year for the predicting artistic success task and both month and year for the short-term wildfire danger forecasting task:

$$\mathbf{v}_i = f(t_i) \in \mathbb{R}^H, \quad (6)$$

where f denotes a learnable function over the input t_i . For the short-term wildfire danger forecasting task, inspired by [63], we adopt a custom encoding with learnable parameters to represent month and year components using both cyclic and linear transformations. Details and results with alternative strategies are provided in Sections D.2 and D.3 of the supplementary material.

Final input embedding. The final embedding $\boldsymbol{\tau}_i$ for a given timestep t_i is obtained by computing the element-wise vector sum of the set representation \mathbf{s}_i , the positional encoding \mathbf{u}_i , and the temporal embedding \mathbf{v}_i :

$$\boldsymbol{\tau}_i = \mathbf{s}_i + \mathbf{u}_i + \mathbf{v}_i \quad (7)$$

The embedding $\boldsymbol{\tau}_i \in \mathbb{R}^H$ is fed forward to a Transformer encoder.

Transformer Encoder. For our Set2Seq Transformer, following [33, 118], we utilize a Transformer encoder module for learning permutation-aware set representations of a sequence $\mathcal{T} \in \mathbb{R}^H$. Throughout this work, we set the number of Transformer encoder blocks (layers) L to 12, the hidden size H to 512, the number of attention heads A to 16, and the feed-forward model size to $2H$. The resulting representations are then passed through two fully connected layers with hidden dimensionality H to generate the final prediction \hat{y} , typically derived from the last timestep. For learning-to-rank tasks, such as the WikiArt-Seq2Rank task for predicting artistic success, we train our methods using a pointwise learning-to-rank objective by minimizing the Mean Squared Error (MSE). For classification tasks, such as short-term wildfire danger forecasting on the Mesogeos dataset, we use the Cross-Entropy (CE) loss. Equations for both objectives are provided in Section A.1 of the supplementary material.

4 Experimental Setup

We evaluate the Set2Seq Transformer on two distinct tasks that require modeling sequences of sets, but differ significantly in modality, structure, and objective. First, we focus on a visual learning-to-rank task of predicting artistic success, introducing the WikiArt-Seq2Rank dataset. We then apply the Set2Seq Transformer to a short-term wildfire danger forecasting task using the Mesogeos dataset [66]. In this section we describe the dataset characteristics, task formulations, baseline methods, and evaluation protocols for each task.

4.1 Predicting Artistic Success

We start by providing specific details about the artistic success prediction task using our novel WikiArt-Seq2Rank dataset. We first formalize the task of predicting artistic success as a visual learning-to-rank problem, then describe the dataset construction, the ranking criteria, train/validation/test splits, baseline methods, and evaluation metrics.

Problem formulation. Given an artist’s body of work as a sequence of sets of artworks created at discrete timesteps, each artist’s career is modeled as a sequence $\{S_1, S_2, \dots, S_T\}$, where S_t denotes the set of artworks created within a discrete time interval t (e.g., a year). Each artwork is encoded as a feature vector using a pretrained visual backbone. The task is formulated as a supervised, pointwise learning-to-rank problem, where the objective is to predict a scalar score y for each artist according to a specific criterion, as shown in Figure 1.

WikiArt-Seq2Rank. For the task of predicting artistic success, we introduce WikiArt-Seq2Rank, a novel dataset that extends the publicly available WikiArt collection [126] by incorporating multiple rankings of 849 renowned visual artists based on various success criteria. The original WikiArt dataset, extensively used in automatic fine-art analysis [19, 39, 40, 89, 111], consists of 75,921 paintings created by 1,111 artists from 1401 up to 2012, spanning major stylistic movements. We omit artworks without a known creation date and artists that have fewer than 10 artworks in the collection. This results in a dataset that consists of 59,458 artworks created by 849 artists. For each artist, we collected information from various publicly available sources to construct rankings based on artist appreciation, grounded in cultural industries theory [10, 100, 125].

Rankings. We compile artist success rankings from various sources, including: (1) eBooks, based on the number of mentions in a corpus of 904 art-related books; (2) The New York Times (NYT), using 4,525 abstracts of art-related reviews from 1981–2019; (3) Wikipedia Mentions and (4) Wikipedia Links, measuring the number of times an artist’s name appears or their page is linked to another artist’s page; (5) Wikipedia Pageviews, tracking the number of times an artist’s page was accessed; (6) Google Ngram, counting mentions of artists in books via Google Books Ngram Viewer (2019 Ed.) [88]; (7) Google Trends, monitoring search frequency in the “painting” category from 2017–2022; (8) Artfacts [4], which ranks artists based on exhibition data; and (9) Artpprice [5], which reports the top 500 artists by auction revenue annually from 2006–2021. We also created an overall ranking, (10) Aggregate Ranking, by aggregating all the individual rankings using the Borda count system [30]. Further details are provided in Section C of the supplementary material.

Train/Val/Test splits. We evaluate our methods using two split strategies: stratified and time series. Each sample represents an artist’s entire career, with static methods using full sets of artworks

and sequential methods using sequences. For the stratified split, the dataset is divided into training (70%), validation (10%), and test (20%) subsets. The time series split assigns artists to training (pre-1930), validation (1930–1951), and test (post-1951) sets, reflecting real-world scenarios. Detailed dataset statistics and results for the time series split are provided in Section C of the supplementary material.

Baseline methods. We compare our Set2Seq Transformer with several static and temporal methods for the task of predicting artistic success. The static baselines include: (1) Vanilla linear regression; (2) Gradient Boosting (XGBoost) [24], an ensemble method for learning-to-rank tasks; (3) DeepSets [138], using mean and max aggregation with a final fully connected layer; and (4) Set Transformer [70]. For temporal baselines, we consider: (5) Hierarchical DeepSets, which first learns representations of individual sets at each timestep and then aggregates these representations across timesteps; (6) LSTM, a bidirectional LSTM [53] with attention [7], using two stacked layers and 512 hidden units; and (7) Transformer [118], which flattens temporal representations and applies positional encoding for each instance. Note that the static methods do not model the temporal structure of artists’ careers, treating the entire body of work as a single unordered set, while the temporal baselines explicitly model the sequence of artwork sets over time. Full implementation details are provided in Section B of the supplementary material.

Evaluation metrics and leaderboard. For evaluation on WikiArt-Seq2Rank, we report Kendall’s τ [64] and Mean Absolute Error (MAE), reflecting performance in rank prediction. Definitions of both metrics are included in Section A.2 of the supplementary material. To aggregate performance across datasets and metrics, we report two leaderboard scores. Inspired by recent advancements in large-scale model evaluation (e.g., Chiang et al. [25]), we first report Bradley–Terry (BT) scores [14], based on pairwise win–loss comparisons between methods across all metric evaluations (cf. Chiang et al. [25] for details on BT scores). Additionally, we report a simple Borda count–based score [27, 98], in which methods are ranked per metric and dataset, and rank-based points are summed to produce a global ordering. Both scores are reported in Table 1 alongside raw metrics.

4.2 Short-Term Wildfire Danger Forecasting

In this section, we describe the short-term wildfire danger forecasting task using the Mesogeos dataset [66]. We begin by formulating the prediction problem and detailing the dataset characteristics. We then introduce a multiple-instance learning (MIL) extension of the task, define an additional setting for evaluating early predictions, and outline the baseline methods and evaluation metrics used in our experiments.

Problem formulation. The task is posed as a binary classification problem, where wildfire danger for a given day is defined as the probability of a fire starting and exceeding 30 hectares, based on fire-driving variables observed over the preceding 30 days. Formally, the input is a temporal sequence of fire-driving observations, which are structured either as single instances or as sets of multiple instances per timestep, and the output is a binary target indicating fire occurrence. Similar to [66], to mitigate the impact of class imbalance, we apply a weighted cross-entropy loss scaled by a logarithmic transformation of fire size.

Mesogeos dataset. The Mesogeos dataset spans the period of 2006–2022 and includes 25,722 samples, of which 8,574 are positive

Table 1: Results for the predicting artistic success task using the WikiArt-Seq2Rank Stratified Split subset. We report Kendall’s τ and Mean Absolute Error (MAE) for different methods and rankings, as well as overall performance in the Aggregate Ranking and leaderboard scores (BT and Borda). PE denotes the use of positional encodings; CE denotes temporal embeddings. (mean) and (max) refer to pooling operations. For Set2Seq Transformer models using Set Transformer only the specific variant is denoted in parentheses. For Kendall’s τ , BT, and Borda, higher (Δ) is better; for MAE, lower (∇) is better. Best results in bold; second best underlined.

Method	Leaderboard		Aggregate Ranking		eBooks		The New York Times		Wikipedia Mentions		Wikipedia Links		Wikipedia Pageviews		Google Ngram		Google Trends		Artfacts		Artprice	
	BT Δ	Borda Δ	τ Δ	MAE ∇	τ Δ	MAE ∇	τ Δ	MAE ∇	τ Δ	MAE ∇	τ Δ	MAE ∇	τ Δ	MAE ∇	τ Δ	MAE ∇	τ Δ	MAE ∇	τ Δ	MAE ∇	τ Δ	MAE ∇
Vanilla (mean)	436	25	0.098	0.734	0.148	0.777	0.076	0.510	0.013	0.444	0.037	0.464	0.132	0.686	0.151	0.681	0.083	0.740	0.090	0.614	0.077	0.919
Vanilla (max)	703	43	0.146	0.520	0.038	0.469	0.075	0.337	0.094	0.284	0.050	0.290	0.121	0.466	0.052	0.653	0.205	0.527	0.236	0.434	0.148	0.515
Gradient Boosting (mean)	1,046	83	0.245	0.229	0.216	0.227	0.125	0.129	0.055	0.113	0.075	0.115	0.145	0.261	0.146	0.283	0.230	0.235	0.450	0.196	0.112	0.252
Gradient Boosting (max)	1,407	195	0.281	0.215	0.306	0.209	0.290	0.093	0.216	0.088	0.234	0.096	0.315	0.221	0.183	0.269	0.316	0.205	0.421	0.208	0.252	0.219
DeepSets (mean)	1,296	152	0.290	0.223	0.308	0.205	0.125	0.100	0.123	0.095	0.201	0.088	0.177	0.249	0.249	0.263	0.120	0.244	0.456	0.190	0.119	0.219
DeepSets (max)	1,837	419	0.411	0.189	0.316	0.179	0.323	0.083	0.262	0.080	0.288	0.076	0.382	0.205	0.296	0.251	0.399	0.178	0.423	0.180	0.230	0.184
Set Transformer (SAB + PMA)	1,404	195	0.374	0.206	0.310	0.183	0.162	0.089	0.184	0.083	0.202	0.098	0.272	0.242	0.214	0.272	0.285	0.208	0.418	0.199	0.227	0.205
Set Transformer (ISAB + PMA)	1,346	169	0.314	0.212	0.299	0.203	0.162	0.088	0.187	0.081	0.198	0.091	0.273	0.232	0.213	0.267	0.233	0.219	0.441	0.196	0.105	0.245
Set Transformer (ISAB + PMA + SAB)	1,293	149	0.314	0.216	0.199	0.237	0.091	0.112	0.213	0.081	0.235	0.087	0.263	0.235	0.168	0.285	0.372	0.186	0.416	0.204	0.095	0.229
Hierarchical DeepSets (max)	1,547	266	0.378	0.201	0.298	0.215	0.275	0.099	0.223	0.088	0.211	0.089	0.307	0.222	0.265	0.259	0.340	0.200	0.478	0.193	0.263	0.215
LSTM (mean)	1,574	282	0.387	0.194	0.323	0.197	0.230	0.088	0.250	0.080	0.298	0.084	0.327	0.211	0.203	0.272	0.330	0.200	0.455	0.189	0.165	0.223
LSTM (max)	1,668	332	0.331	0.204	0.431	0.179	0.143	0.103	0.290	0.077	0.284	0.081	0.335	0.215	0.247	0.254	0.331	0.193	0.395	0.181	0.305	0.189
Transformer w/o PE + CE	1,577	286	0.354	0.199	0.329	0.203	0.150	0.089	0.253	0.078	0.252	0.083	0.336	0.210	0.178	0.281	0.283	0.208	0.496	0.174	0.236	0.211
Transformer + PE	1,619	304	0.344	0.207	0.322	0.205	0.246	0.089	0.286	0.077	0.242	0.080	0.347	0.209	0.203	0.279	0.307	0.200	0.474	0.173	0.249	0.210
Transformer + CE	1,516	248	0.281	0.221	0.333	0.200	0.215	0.088	0.279	0.078	0.287	0.079	0.244	0.247	0.177	0.282	0.378	0.183	0.441	0.179	0.083	0.215
Transformer + PE + CE	1,752	378	0.346	0.169	0.386	0.189	0.265	0.088	0.303	0.073	0.336	0.076	0.323	0.220	0.201	0.272	0.339	0.181	0.478	0.181	0.314	0.204
Set2Seq LSTM (DeepSets - mean)	1,604	298	0.204	0.237	0.322	0.178	0.208	0.083	0.284	0.075	0.250	0.080	0.308	0.224	0.242	0.267	0.346	0.184	0.451	0.182	0.204	0.208
Set2Seq LSTM (DeepSets - max)	1,716	361	0.319	0.213	0.296	0.186	0.304	0.082	0.296	0.074	0.320	0.079	0.318	0.228	0.255	0.262	0.352	0.180	0.420	0.193	0.268	0.188
Set2Seq LSTM (SAB + PMA)	1,718	359	0.294	0.213	0.387	0.175	0.281	0.085	0.261	0.075	0.324	0.082	0.304	0.231	0.314	0.239	0.352	0.185	0.419	0.186	0.290	0.194
Set2Seq LSTM (ISAB + PMA)	1,609	306	0.189	0.234	0.389	0.175	0.112	0.085	0.252	0.075	0.287	0.086	0.281	0.239	0.257	0.254	0.293	0.200	0.459	0.185	0.226	0.191
Set2Seq LSTM (ISAB + PMA + SAB)	1,542	267	0.295	0.217	0.338	0.184	0.229	0.089	0.301	0.074	0.165	0.088	0.235	0.241	0.290	0.250	0.319	0.208	0.457	0.193	0.211	0.213
Set2Seq Transformer (DeepSets - mean)	1,711	360	0.376	0.203	0.362	0.185	0.234	0.090	0.267	0.074	0.314	0.079	0.275	0.250	0.281	0.260	0.367	0.192	0.462	0.174	0.261	0.191
Set2Seq Transformer (DeepSets - max)	1,844	425	0.383	0.205	0.411	0.175	0.197	0.084	0.256	0.076	0.310	0.081	0.354	0.205	0.285	0.251	0.387	0.182	0.474	0.176	0.283	0.189
Set2Seq Transformer (SAB + PMA)	1,782	398	0.425	0.187	0.347	0.180	0.296	0.084	0.296	0.080	0.316	0.081	0.344	0.213	0.231	0.261	0.350	0.199	0.476	0.186	0.250	0.181
Set2Seq Transformer (ISAB + PMA)	1,857	423	0.414	0.184	0.406	0.174	0.277	0.084	0.288	0.071	0.310	0.084	0.288	0.233	0.303	0.252	0.390	0.184	0.493	0.180	0.282	0.191
Set2Seq Transformer (ISAB + PMA + SAB)	1,598	297	0.360	0.202	0.369	0.198	0.191	0.086	0.275	0.080	0.294	0.080	0.274	0.231	0.243	0.263	0.348	0.197	0.453	0.190	0.189	0.212

fire cases and 17,148 are negative. The data is split temporally into training (2006–2019), validation (2020), and test (2021–2022) sets. Each sample corresponds to a 30-day period and includes dynamic features (e.g., vegetation indices and weather variables) normalized over time, as well as static geographical features (e.g., topography and elevation), repeated across the sequence. Additional details on dataset characteristics and preprocessing are provided in Section D of the supplementary material.

Single-instance and multiple-instance learning settings. Originally structured for single-instance learning, where each sample consists of 30 daily observations, we extend Mesogeo to support multiple-instance learning via temporal grouping. Observations are aggregated into fixed-size sets, resulting in five input configurations: (a) thirty 1-day sets, (b) fifteen 2-day sets, (c) ten 3-day sets, (d) six 5-day sets, and (e) three 10-day sets. Each configuration spans the full 30-day period, and the input to the model is a sequence of sets of fire-driving variables. The objective is to predict the probability of a fire event on the final day based on the full 30-day input.

Early short-term wildfire danger forecasting task. To simulate realistic forecasting conditions, we define an early short-term wildfire danger forecasting task, where models predict wildfire occurrence at progressively earlier timesteps with limited temporal context. For each input configuration consisting of l timesteps, the model receives a sequence of k sets and is evaluated at each timestep $t \in 1, \dots, l$ based only on input available up to timestep t . This setup enables us to assess model performance under incomplete information and track how predictive accuracy evolves as more temporal context becomes available. Note that for this task, we use the Set2Seq Transformer with the Set Transformer (ISAB + PMA) module as its set-based variant.

Baseline methods. We compare our Set2Seq Transformer against several baselines that reflect different modeling assumptions. For set-based methods, we include: (1) DeepSets [138], with max pooling;

and (2) Set Transformer [70], using ISAB and PMA modules. For temporal modeling, we consider: (3) a bidirectional LSTM [7, 53] with two stacked layers and 512 hidden units; and (4) a Transformer encoder [118], which flattens instance-level representations over time and applies positional encodings. For the Set2Seq Transformer, we report results using two variants: one with DeepSets (max pooling) and one with Set Transformer (ISAB + PMA) as the set-based component.

Evaluation metrics. We report Precision–Recall Area Under the Curve (PR-AUC) [43] and F1-score, both commonly used in high-risk event forecasting. Detailed definitions of both metrics are included in Section A.2 of the supplementary material.

5 Experimental Results

In this section, we present the experimental results for the predicting artistic success and the short-term wildfire danger forecasting tasks.

5.1 Predicting Artistic Success

The main results of the evaluation of our methods using the WikiArt-Seq2Rank dataset are summarized in Table 1. For improved clarity, the second column reports the leaderboard BT and Borda scores, which summarize method comparisons across all evaluation settings. The third column shows performance on the Aggregate Ranking, constructed by aggregating the individual success rankings into a single ranking, as mentioned in Section 4.1.

Performance of static methods. Max pooling improves most static baselines by leveraging salient features from the ResNet-34 backbone. DeepSets and Set Transformer outperform Vanilla and Gradient Boosting baselines across most settings. We have to note that DeepSets with max pooling comprise a very strong baseline performing almost on-par with both temporal-based baseline methods and our Set2Seq framework across all rankings, while achieving best

Table 2: F1-Score and Precision-Recall Area Under Curve (PR-AUC) for different methods for the short-term wildfire danger forecasting task using Mesogeos [66]. PE denotes utilizing position encodings. CE denotes utilizing temporal embeddings. k denotes the number of instances for a set \mathcal{S} at timestep t . l denotes the number of timesteps t for a sequence \mathcal{T} . For both metrics higher is better. Best results in bold; second best underlined.

Method	$k=1, l=30$		$k=2, l=15$		$k=3, l=10$		$k=5, l=6$		$k=10, l=3$	
	F1	PR-AUC								
DeepSets	0.724	0.794	0.692	0.769	0.699	0.769	0.692	0.770	0.706	0.784
SetTransformer	0.731	0.798	0.721	0.781	0.719	0.781	0.720	0.780	0.716	0.781
LSTM	0.777	0.856	0.762	0.844	0.765	0.845	0.762	0.833	0.744	0.814
Transformer + PE	0.788	0.851	<u>0.777</u>	0.843	0.762	0.842	0.762	0.828	<u>0.754</u>	0.824
Set2Seq Transformer (Deep Sets) + PE	0.771	0.855	0.773	0.856	<u>0.768</u>	0.846	<u>0.764</u>	<u>0.836</u>	0.749	0.826
Set2Seq Transformer (Deep Sets) + PE + CE	<u>0.784</u>	0.864	0.761	0.863	<u>0.768</u>	0.833	0.756	0.830	0.747	<u>0.834</u>
Set2Seq Transformer (ISAB + PMA) + PE	0.776	<u>0.865</u>	0.772	0.848	0.741	<u>0.851</u>	0.755	0.832	0.736	0.816
Set2Seq Transformer (ISAB + PMA) + PE + CE	<u>0.784</u>	0.866	0.783	<u>0.861</u>	0.772	0.856	0.771	0.850	0.761	0.835

results in several cases. Nevertheless, the performance of Hierarchical DeepSets is consistently inferior, indicating that DeepSets can leverage the sufficient information in larger static sets, while not being able to model positional and temporal aspects.

Performance of temporal methods. Table 1 shows that leveraging temporal information improves performance on WikiArt-Seq2Rank, with both bidirectional LSTMs and Transformers outperforming static baselines. Similar to our static methods, maximum pooling at the set-level improves the performance of our bidirectional LSTM baselines across almost all rankings. Finally, it can be clearly seen that our Transformer baseline is the strongest temporal-based baseline method especially when combined with both positional encodings and temporal embeddings.

Set2Seq Transformer improves the performance of static methods and outperforms temporal-based baselines. Our proposed Set2Seq Transformer outperforms almost all baselines across the different rankings and on average. It can be clearly seen that the Set2Seq framework demonstrates notable improvements over set-based static methods by effectively modeling the temporal dimension. It is also worth noting that our Set2Seq Transformer generally outperforms temporal-based baselines across different settings. In particular, it achieves the best performance on the Aggregate Ranking, confirming its consistent advantage across different criteria of artistic success.

Performance based on different rankings. We observe variation in the performance of our methods across different rankings. That is expected since these rankings differ based on the criteria that they incorporate. Additionally, the number of relevant artists in different rankings and other minor effects based on, e.g., ties, have a significant impact in the performance of our evaluated methods. However, our Set2Seq Transformer maintains consistently strong results across the board, while outperforming almost all baseline methods in the Aggregate Ranking.

Position-aware encoding and temporal embeddings significantly improve performance. We observe that combining position-aware encoding and temporal embeddings notably enhances Transformer performance across variants. Another important observation is that Transformers consistently outperform the Bi-LSTM methods across all different rankings. Additionally, we

observe that in our Set2Seq framework Transformer-based methods outperform their bidirectional LSTM counterpart.

Performance on leaderboard. Table 1 also reports two aggregate leaderboard scores—the Bradley-Terry (BT) score and a Borda count-based score—which summarize performance across all rankings and evaluation metrics. The Set2Seq Transformer achieves the highest scores under both schemes, indicating consistent improvements over static and temporal baselines. Interestingly, DeepSets with max pooling also ranks highly, suggesting that the aggregated set of artworks may already contain strong expressive cues about artistic success, even without temporal modeling. However, the performance of Hierarchical DeepSets is once again significantly worse than that of all temporal-based baselines, highlighting the limitations of shallow temporal aggregation and the importance of explicitly modeling positional and sequential dependencies. Additional results for the predicting artistic success task, including results for the WikiArt-Seq2Rank Time Series Split, using alternative visual backbones, and qualitative analysis, are provided in Section C of the supplementary material.

5.2 Short-Term Wildfire Danger Forecasting

Table 2 summarizes the main results of our methods on the Mesogeos dataset for short-term wildfire forecasting.

Performance on sequential single-instance learning. Table 2 presents results for sequential single-instance (i.e., $k=1$) and multiple-instance learning, alongside LSTM and Transformer baselines re-implemented to align with Mesogeos [66]. Static methods, such as DeepSets and Set Transformer, which do not account for temporality, are significantly outperformed by sequential alternatives, with our Set2Seq Transformer consistently surpassing most baseline models. Notably, the Set2Seq Transformer performs strongly in single-instance learning, outperforming sequential methods that process raw input signals without transforming them into sets. This result indicates that our Set2Seq Transformer can effectively handle sets of single instances while maintaining high performance.

Sensitivity analysis on sequential multiple-instance learning. To simulate real-world conditions with noisy or multi-day observations, we created a controlled setting by grouping consecutive

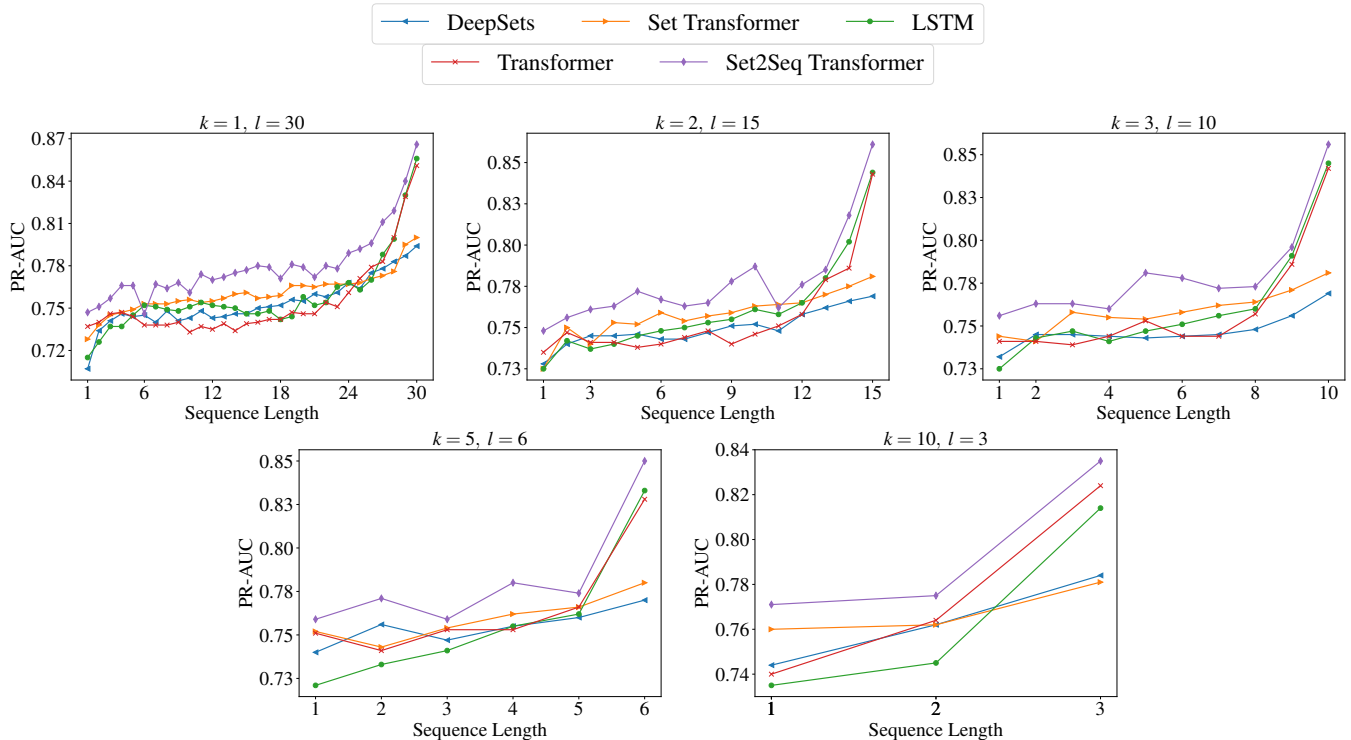


Figure 3: Performance on early short-term wildfire danger forecasting using Mesogeos [66]. Given progressively earlier timesteps and limited temporal context, the task is to predict wildfire danger with incomplete information. PR-AUC scores are reported for various models and settings across different sequence lengths.

days using a sliding time window. For this task, we evaluated Hierarchical DeepSets and Set Transformer baselines, which first learn set representations per timestep and then aggregate them across timesteps. As shown in Table 2, our Set2Seq Transformer (ISAB + PMA) utilizing position encodings and temporal embeddings, consistently outperforms most baselines in this setting. The model adapts well to varying sequence lengths and set sizes, with positional and temporal representations significantly improving PR-AUC scores, underscoring the model’s effectiveness for short-term wildfire forecasting. Overall, our Set2Seq Transformer effectively integrates set, positional, and temporal representations, outperforming baselines and generalizing across modalities and tasks.

Early short-term wildfire danger forecasting. In contrast to the standard forecasting setup in Table 2, which assumes full 30-day context, Figure 3 presents results for a proactive early forecasting task. In this setting, models predict wildfire occurrence on day 31 based on progressively increasing input context, starting from day 1 and adding observations incrementally up to the full 30-day window. Across the five temporal configurations, this results in a total of 64 experiments. As mentioned in Section 4.2, we use the Set2Seq Transformer with the Set Transformer (ISAB + PMA) module in this setup. Figure 3 shows that our Set2Seq Transformer outperforms all baselines in 62 out of 64 cases, demonstrating its robustness under limited context and its ability to model temporal dependencies effectively. Static set-based methods, such as DeepSets and Set Transformer,

perform comparably to temporal models at early timesteps, where limited context diminishes the benefits of temporal modeling. However, unlike temporal baselines, their performance plateaus as more timesteps are added. In contrast, dynamic models—including LSTM, Transformer, and Set2Seq—exhibit significant performance gains when later timesteps become available, highlighting their ability to exploit evolving patterns in the input sequence. Additional ablation studies, including Set Transformer variants and temporal encoding strategies, are provided in Section D of the supplementary material.

6 Conclusion

We propose Set2Seq Transformer, a novel method for learning temporal position-aware representations of sequences of sets. Quantitative results using two distinct datasets, WikiArt-Seq2Rank, a newly curated dataset introduced here for predicting artistic success, and Mesogeos for short-term wildfire danger forecasting, demonstrate that our Set2Seq Transformer outperforms strong static and temporal methods for efficient sequential multiple-instance learning, while effectively capturing essential temporal information. Our findings underscore the importance of jointly modeling permutation-invariant structure within sets and temporal dynamics across sequences—an essential, but often underexplored aspect of many real-world applications, where capturing both the internal structure of sets and their temporal relationships is crucial for modeling complex patterns.

References

- [1] Tatiana Acero-Cuellar, Federica Bianco, Gregory Dobler, Masao Sako, Helen Qu, and The LSST Dark Energy Science Collaboration. 2023. What's the Difference? The Potential for Convolutional Neural Networks for Transient Detection without Template Subtraction. *The Astronomical Journal* 166, 3 (aug 2023), 115. doi:10.3847/1538-3881/ace9d8
- [2] Panos Achlioptas, Maks Ovsjanikov, Kilichbek Haydarov, Mohamed Elhoseiny, and Leonidas J. Guibas. 2021. ArtEmis: Affective Language for Visual Art. In *Proceedings of the IEEE/CVF Conference on Computer Vision and Pattern Recognition (CVPR)*. 11569–11579.
- [3] Jordan Anaya, John-William Sidhom, Faisal Mahmood, and Alexander Baras. 2023. Multiple-instance learning of somatic mutations for the classification of tumour type and the prediction of microsatellite status. *Nature Biomedical Engineering* 8 (11 2023), 1–11. doi:10.1038/s41551-023-01120-3
- [4] Artfacts. [n. d.]. Home of the Artist Ranking. <https://artfacts.net/>
- [5] Artprice. [n. d.]. Art market, auction sales and artists' prices and indices - Artprice, the world leader of art market information. <https://www.artprice.com/>
- [6] Javed A. Aslam and Mark Montague. 2001. Models for metasearch. In *Proceedings of the 24th Annual International ACM SIGIR Conference on Research and Development in Information Retrieval* (New Orleans, Louisiana, USA) (SIGIR '01). Association for Computing Machinery, New York, NY, USA, 276–284. doi:10.1145/383952.384007
- [7] Dzmitry Bahdanau, Kyunghyun Cho, and Yoshua Bengio. 2014. Neural machine translation by jointly learning to align and translate. *arXiv preprint arXiv:1409.0473* (2014).
- [8] Zechen Bai, Yuta Nakashima, and Noa Garcia. 2021. Explain Me the Painting: Multi-Topic Knowledgeable Art Description Generation. In *2021 IEEE/CVF International Conference on Computer Vision (ICCV)*. 5402–5412. doi:10.1109/ICCV48922.2021.00537
- [9] Ada-Astrid Balauca, Danda Pani Paudel, Kristina Toutanova, and Luc Van Gool. 2025. Taming CLIP for Fine-Grained and Structured Visual Understanding of Museum Exhibits. In *Computer Vision – ECCV 2024*, Aleš Leonardis, Elisa Ricci, Stefan Roth, Olga Russakovsky, Torsten Sattler, and Gül Varol (Eds.). Springer Nature Switzerland, Cham, 377–394.
- [10] Mitali Banerjee, Benjamin M. Cole, and Paul Ingram. 2023. “Distinctive from What? And for Whom?” Deep Learning-Based Product Distinctiveness, Social Structure, and Third-Party Certifications. *Academy of Management Journal* 66, 4 (2023), 1016–1041. doi:10.5465/amj.2021.0175 arXiv:<https://doi.org/10.5465/amj.2021.0175>
- [11] Somnath Basu Roy Chowdhury, Faeze Brahmam, and Snigdha Chaturvedi. 2021. Is Everything in Order? A Simple Way to Order Sentences. In *Proceedings of the 2021 Conference on Empirical Methods in Natural Language Processing*, Marie-Francine Moens, Xuanjing Huang, Lucia Specia, and Scott Wen-tau Yih (Eds.). Association for Computational Linguistics, Online and Punta Cana, Dominican Republic, 10769–10779. doi:10.18653/v1/2021.emnlp-main.841
- [12] Austin R. Benson, Ravi Kumar, and Andrew Tomkins. 2018. Sequences of Sets. In *Proceedings of the 24th ACM SIGKDD International Conference on Knowledge Discovery & Data Mining* (London, United Kingdom) (KDD '18). Association for Computing Machinery, New York, NY, USA, 1148–1157. doi:10.1145/3219819.3220100
- [13] Yi Bin, Wenhao Shi, Yujuan Ding, Zhiqiang Hu, Zheng Wang, Yang Yang, See-Kiong Ng, and Heng Tao Shen. 2024. GalleryGPT: Analyzing Paintings with Large Multimodal Models. In *Proceedings of the 32nd ACM International Conference on Multimedia* (Melbourne VIC, Australia) (MM '24). Association for Computing Machinery, New York, NY, USA, 7734–7743.
- [14] Ralph Allan Bradley and Milton E. Terry. 1952. Rank Analysis of Incomplete Block Designs: I. The Method of Paired Comparisons. *Biometrika* 39, 3/4 (1952), 324–345.
- [15] Tom Brown, Benjamin Mann, Nick Ryder, Melanie Subbiah, Jared D Kaplan, Prafulla Dhariwal, Arvind Neelakantan, Pranav Shyam, Girish Sastry, Amanda Askell, Sandhini Agarwal, Ariel Herbert-Voss, Gretchen Krueger, Tom Henighan, Rewon Child, Aditya Ramesh, Daniel Ziegler, Jeffrey Wu, Clemens Winter, Chris Hesse, Mark Chen, Eric Sigler, Mateusz Litwin, Scott Gray, Benjamin Chess, Jack Clark, Christopher Berner, Sam McCandlish, Alec Radford, Ilya Sutskever, and Dario Amodei. 2020. Language Models are Few-Shot Learners. In *Advances in Neural Information Processing Systems*, H. Larochelle, M. Ranzato, R. Hadsell, M.F. Balcan, and H. Lin (Eds.), Vol. 33. Curran Associates, Inc., 1877–1901. https://proceedings.neurips.cc/paper_files/paper/2020/file/1457c0d6bfc4967418bfb8ac142f64a-Paper.pdf
- [16] C. Cammalleri, J. V. Vogt, B. Bisselink, and A. de Roo. 2017. Comparing soil moisture anomalies from multiple independent sources over different regions across the globe. *Hydrology and Earth System Sciences* 21, 12 (2017), 6329–6343. doi:10.5194/hess-21-6329-2017
- [17] Zhe Cao, Tao Qin, Tie-Yan Liu, Ming-Feng Tsai, and Hang Li. 2007. Learning to rank: from pairwise approach to listwise approach. In *Proceedings of the 24th International Conference on Machine Learning* (Corvallis, Oregon, USA) (ICML '07). Association for Computing Machinery, New York, NY, USA, 129–136. doi:10.1145/1273496.1273513
- [18] Giovanna Castellano, Vincenzo Digeno, Giovanni Sansaro, and Gennaro Vessio. 2022. Leveraging Knowledge Graphs and Deep Learning for automatic art analysis. *Knowledge-Based Systems* 248 (2022), 108859. doi:10.1016/j.knsys.2022.108859
- [19] Eva Cetinic, Tomislav Lipic, and Sonja Grgic. 2019. A deep learning perspective on beauty, sentiment, and remembrance of art. *IEEE Access* 7 (2019), 73694–73710.
- [20] Eva Cetinic, Tomislav Lipic, and Sonja Grgic. 2020. Learning the Principles of Art History with convolutional neural networks. *Pattern Recognition Letters* 129 (2020), 56 – 62. doi:10.1016/j.patrec.2019.11.008
- [21] Eva Cetinic and James She. 2021. Understanding and Creating Art with AI: Review and Outlook. *arXiv preprint arXiv:2102.09109* (2021).
- [22] R. Qi Charles, Hao Su, Mo Kaichun, and Leonidas J. Guibas. 2017. PointNet: Deep Learning on Point Sets for 3D Classification and Segmentation. In *2017 IEEE Conference on Computer Vision and Pattern Recognition (CVPR)*. 77–85. doi:10.1109/CVPR.2017.16
- [23] Shixing Chen, Caojin Zhang, Ming Dong, Jialiing Le, and Mike Rao. 2017. Using Ranking-CNN for Age Estimation. In *2017 IEEE Conference on Computer Vision and Pattern Recognition (CVPR)*. 742–751. doi:10.1109/CVPR.2017.86
- [24] Tianqi Chen and Carlos Guestrin. 2016. XGBoost: A Scalable Tree Boosting System. In *Proceedings of the 22nd ACM SIGKDD International Conference on Knowledge Discovery and Data Mining* (San Francisco, California, USA) (KDD '16). Association for Computing Machinery, New York, NY, USA, 785–794. doi:10.1145/2939672.2939785
- [25] Wei-Lin Chiang, Lianmin Zheng, Ying Sheng, Anastasios N. Angelopoulos, Tianle Li, Dacheng Li, Banghua Zhu, Hao Zhang, Michael I. Jordan, Joseph E. Gonzalez, and Ion Stoica. 2024. Chatbot arena: an open platform for evaluating LLMs by human preference. In *Proceedings of the 41st International Conference on Machine Learning* (Vienna, Austria) (ICML '24). JMLR.org, Article 331, 30 pages.
- [26] Junyoung Chung, Caglar Gulcehre, KyungHyun Cho, and Yoshua Bengio. 2014. Empirical evaluation of gated recurrent neural networks on sequence modeling. *arXiv preprint arXiv:1412.3555* (2014).
- [27] Pierre Colombo, Nathan Noiry, Ekhine Irurozki, and Stephan CLEMENCON. 2022. What are the best Systems? New Perspectives on NLP Benchmarking. In *Advances in Neural Information Processing Systems*, Alice H. Oh, Alekh Agarwal, Danielle Belgrave, and Kyunghyun Cho (Eds.).
- [28] Copernicus Climate Change Service. 2019. Land cover classification gridded maps from 1992 to present derived from satellite observation. doi:10.24381/cds.006f2c9a Accessed on 21-11-2024.
- [29] James E. Cutting, Jordan E. DeLong, and Christine E. Nothelfer. 2010. Attention and the Evolution of Hollywood Film. *Psychological Science* 21, 3 (2010), 432–439. doi:10.1177/0956797610361679 arXiv:<https://doi.org/10.1177/0956797610361679> PMID: 20424081.
- [30] Jean-Charles de Borda. 1781. Mémoire sur les élections au scrutin. *Histoire de l'Académie Royale des Sciences* (1781).
- [31] J. Deng, W. Dong, R. Socher, L.-J. Li, K. Li, and L. Fei-Fei. 2009. ImageNet: A Large-Scale Hierarchical Image Database. In *CVPR09*.
- [32] Yingying Deng, Fan Tang, Weiming Dong, Chongyang Ma, Xingjia Pan, Lei Wang, and Changsheng Xu. 2022. StyTr2: Image Style Transfer With Transformers. In *Proceedings of the IEEE/CVF Conference on Computer Vision and Pattern Recognition (CVPR)*. 11326–11336.
- [33] Jacob Devlin, Ming-Wei Chang, Kenton Lee, and Kristina Toutanova. 2019. BERT: Pre-training of Deep Bidirectional Transformers for Language Understanding. In *Proceedings of the 2019 Conference of the North American Chapter of the Association for Computational Linguistics: Human Language Technologies, Volume 1 (Long and Short Papers)*. Association for Computational Linguistics, Minneapolis, Minnesota, 4171–4186. doi:10.18653/v1/N19-1423
- [34] K. Didan. 2015. MOD13A2 MODIS/Terra Vegetation Indices 16-Day L3 Global 1km SIN Grid V006 [Data set]. doi:10.5067/MODIS/MOD13A2.006 Accessed 2024-11-21.
- [35] Thomas G. Dietterich, Richard H. Lathrop, and Tomás Lozano-Pérez. 1997. Solving the multiple instance problem with axis-parallel rectangles. *Artificial Intelligence* 89, 1 (1997), 31–71. doi:10.1016/S0004-3702(96)00034-3
- [36] Alexey Dosovitskiy, Lucas Beyer, Alexander Kolesnikov, Dirk Weissenborn, Xiaohua Zhai, Thomas Unterthiner, Mostafa Dehghani, Matthias Minderer, Georg Heigold, Sylvain Gelly, Jakob Uzkoreit, and Neil Houlsby. 2021. An Image is Worth 16x16 Words: Transformers for Image Recognition at Scale. In *International Conference on Learning Representations*. <https://openreview.net/forum?id=YicbFdNTTy>
- [37] Cora Dvorkin, Siddharth Mishra-Sharma, Brian Nord, V Ashley Villar, Camille Avestruz, Keith Bechtol, Aleksandra Ciprijanović, Andrew J Connolly, Lehman H Garrison, Gautham Narayan, et al. 2022. Machine learning and cosmology. *arXiv preprint arXiv:2203.08056* (2022).
- [38] Cynthia Dwork, Ravi Kumar, Moni Naor, and D. Sivakumar. 2001. Rank aggregation methods for the Web. In *Proceedings of the 10th International Conference on World Wide Web* (Hong Kong, Hong Kong) (WWW '01). Association for Computing Machinery, New York, NY, USA, 613–622. doi:10.1145/371920.372165
- [39] Athanasios Efthymiou, Stevan Rudinac, Monika Kackovic, Marcel Worring, and Nachoem Wijnberg. 2021. Graph Neural Networks for Knowledge Enhanced Visual Representation of Paintings. In *Proceedings of the 29th ACM International*

- Conference on Multimedia (Virtual Event, China) (MM '21). Association for Computing Machinery, New York, NY, USA, 3710–3719. doi:10.1145/3474085.3475586
- [40] Ahmed Elgammal, Bingchen Liu, Diana Kim, Mohamed Elhoseiny, and Marian Mazonne. 2018. The shape of art history in the eyes of the machine. In *Proceedings of the Thirty-Second AAAI Conference on Artificial Intelligence and Thirtieth Innovative Applications of Artificial Intelligence Conference and Eighth AAAI Symposium on Educational Advances in Artificial Intelligence* (New Orleans, Louisiana, USA) (AAAI'18/IAAI'18/EAAI'18). AAAI Press, Article 266, 9 pages.
- [41] European Space Agency and Airbus. 2022. Copernicus DEM. Title of the publication associated with this dataset: Copernicus DEM.
- [42] Heng Fang, Sheng Huang, Wenhao Tang, Luwen Huangfu, and Bo Liu. 2024. SAM-MIL: A Spatial Contextual Aware Multiple Instance Learning Approach for Whole Slide Image Classification. In *ACM Multimedia 2024*.
- [43] Tom Fawcett. 2006. An introduction to ROC analysis. *Pattern Recognition Letters* 27, 8 (2006), 861–874. doi:10.1016/j.patrec.2005.10.010 ROC Analysis in Pattern Recognition.
- [44] Samuel P Fraiberger, Roberta Sinatra, Magnus Resch, Christoph Riedl, and Albert-László Barabási. 2018. Quantifying reputation and success in art. *Science* 362, 6416 (2018), 825–829.
- [45] Noa Garcia, Benjamin Renoust, and Yuta Nakashima. 2019. Context-Aware Embeddings for Automatic Art Analysis. In *Proceedings of the 2019 on International Conference on Multimedia Retrieval* (Ottawa ON, Canada) (ICMR '19). Association for Computing Machinery, New York, NY, USA, 25–33. doi:10.1145/3323873.3325028
- [46] Jonas Gehring, Michael Auli, David Grangier, Denis Yarats, and Yann N. Dauphin. 2017. Convolutional sequence to sequence learning. In *Proceedings of the 34th International Conference on Machine Learning - Volume 70* (Sydney, NSW, Australia) (ICML '17). JMLR.org, 1243–1252.
- [47] Getty Publications. [n. d.]. Getty Publications - Books on Art | Getty. <https://www.getty.edu/publications/>
- [48] Google Trends. [n. d.]. See what's trending across Google Search, Google News and YouTube. <https://trends.google.com/trends/>
- [49] Alex Graves. 2012. *Supervised Sequence Labelling with Recurrent Neural Networks*. Vol. 385. doi:10.1007/978-3-642-24797-2
- [50] Guggenheim Publications. [n. d.]. Guggenheim publications are renowned for the high quality of their design and production, as well as for the depth of their scholarship. <https://www.guggenheim.org/publications/>
- [51] Yulan Guo, Hanyun Wang, Qingyong Hu, Hao Liu, Li Liu, and Mohammed Benamoun. 2021. Deep Learning for 3D Point Clouds: A Survey. *IEEE Trans. Pattern Anal. Mach. Intell.* 43, 12 (dec 2021), 4338–4364. doi:10.1109/TPAMI.2020.3005434
- [52] Kaiming He, Xiangyu Zhang, Shaoqing Ren, and Jian Sun. 2016. Deep Residual Learning for Image Recognition. In *Proceedings of the IEEE Conference on Computer Vision and Pattern Recognition (CVPR)*.
- [53] Sepp Hochreiter and Jürgen Schmidhuber. 1997. Long Short-Term Memory. *Neural Comput.* 9, 8 (nov 1997), 1735–1780. doi:10.1162/neco.1997.9.8.1735
- [54] M. Honnibal, I. Montani, Van Landeghem S., and A. Boyd. 2020. spaCy: industrial-strength natural language processing in Python. <https://doi.org/10.5281/zenodo.1212303>.
- [55] Zhiyuan Hu, Jia Jia, Bei Liu, Yaohua Bu, and Jianlong Fu. 2020. Aesthetic-Aware Image Style Transfer. In *Proceedings of the 28th ACM International Conference on Multimedia* (Seattle, WA, USA) (MM '20). Association for Computing Machinery, New York, NY, USA, 3320–3329. doi:10.1145/3394171.3413853
- [56] Maximilian Ilse, Jakub Tomczak, and Max Welling. 2018. Attention-based Deep Multiple Instance Learning. In *Proceedings of the 35th International Conference on Machine Learning (Proceedings of Machine Learning Research, Vol. 80)*, Jennifer Dy and Andreas Krause (Eds.). PMLR, 2127–2136. <https://proceedings.mlr.press/v80/ilse18a.html>
- [57] Thorsten Joachims. 2002. Optimizing search engines using clickthrough data. In *Proceedings of the Eighth ACM SIGKDD International Conference on Knowledge Discovery and Data Mining* (Edmonton, Alberta, Canada) (KDD '02). Association for Computing Machinery, New York, NY, USA, 133–142. doi:10.1145/775047.775067
- [58] Matthew L. Jockers. 2013. *Macroanalysis: Digital Methods and Literary History*. University of Illinois Press. doi:10.5406/illinois/9780252037528.001.0001
- [59] Mateusz Jurewicz and Leon Derczynski. 2021. Set-to-Sequence Methods in Machine Learning: A Review. *J. Artif. Int. Res.* 71 (sep 2021), 885–924. doi:10.1613/jair.1.12839
- [60] Mateusz Jurewicz and Leon Derczynski. 2022. Set Interdependence Transformer: Set-to-Sequence Neural Networks for Permutation Learning and Structure Prediction. In *Proceedings of the Thirty-First International Joint Conference on Artificial Intelligence, IJCAI-22*, Lud De Raedt (Ed.). International Joint Conferences on Artificial Intelligence Organization, 3128–3134. doi:10.24963/ijcai.2022/434 Main Track.
- [61] Nal Kalchbrenner and Phil Blunsom. 2013. Recurrent Continuous Translation Models. In *Proceedings of the 2013 Conference on Empirical Methods in Natural Language Processing*, David Yarowsky, Timothy Baldwin, Anna Korhonen, Karen Livescu, and Steven Bethard (Eds.). Association for Computational Linguistics, Seattle, Washington, USA, 1700–1709. <https://aclanthology.org/D13-1176>
- [62] Jakob Nikolas Kather, Alexander T. Pearson, Niels Halama, Dirk Jäger, Jeremias Krause, Sven Heiko Loosen, Alexander Marx, Peter Boor, Frank Tacke, Ulf Peter Neumann, Heike Irmgard Grabsch, Takaki Yoshikawa, Hermann Brenner, Jenny Chang-Claude, Michael Hoffmeister, Christian Trautwein, and Tom Luedde. 2019. Deep learning can predict microsatellite instability directly from histology in gastrointestinal cancer. *Nature Medicine* 25 (2019), 1054–1056. <https://api.semanticscholar.org/CorpusID:173994116>
- [63] Seyed Mehran Kazemi, Rishab Goel, Sepehr Eghbali, Janahan Ramanan, Jaspreet Sahota, Sanjay Thakur, Stella Wu, Cathal Smyth, Pascal Poupart, and Marcus Brubaker. 2019. Time2vec: Learning a vector representation of time. *ArXiv preprint arXiv:1907.05321* (2019).
- [64] M. G. Kendall. 1938. A New Measure of Rank Correlation. *Biometrika* 30, 1/2 (1938), 81–93. <http://www.jstor.org/stable/2332226>
- [65] Diana S. Kim, Bingchen Liu, Ahmed Elgammal, and Marian Mazonne. 2018. Finding Principal Semantics of Style in Art. In *2018 IEEE 12th International Conference on Semantic Computing (ICSC)*. 156–163. doi:10.1109/ICSC.2018.00030
- [66] Spyros Kondylatos, Ioannis Prapas, Gustav Camps-Valls, and Ioannis Papoutsis. 2023. Mesogeos: A multi-purpose dataset for data-driven wildfire modeling in the Mediterranean. In *Thirty-seventh Conference on Neural Information Processing Systems Datasets and Benchmarks Track*. <https://openreview.net/forum?id=VH1vxapUTs>
- [67] Iryna Korshunova, Jonas Degraeve, Ferenc Huszar, Yarin Gal, Arthur Gretton, and Joni Dambre. 2018. BRUNO: A Deep Recurrent Model for Exchangeable Data. In *Advances in Neural Information Processing Systems*, S. Bengio, H. Wallach, H. Larochelle, K. Grauman, N. Cesa-Bianchi, and R. Garnett (Eds.), Vol. 31. Curran Associates, Inc. https://proceedings.neurips.cc/paper_files/paper/2018/file/1b9f38268c50805669fd8caf8f3cc84a-Paper.pdf
- [68] Pawan Kumar, Dhanajit Brahma, Harish Karnick, and Piyush Rai. 2020. Deep Attentive Ranking Networks for Learning to Order Sentences. *Proceedings of the AAAI Conference on Artificial Intelligence* 34, 05 (Apr. 2020), 8115–8122. doi:10.1609/aaai.v34i05.6323
- [69] Mirella Lapata. 2006. Automatic Evaluation of Information Ordering: Kendall's Tau. *Computational Linguistics* 32, 4 (12 2006), 471–484. doi:10.1162/coli.2006.32.4.471 arXiv:https://direct.mit.edu/coli/article-pdf/32/4/471/1798347/coli.2006.32.4.471.pdf
- [70] Juho Lee, Yoonho Lee, Jungtaek Kim, Adam Kosiorek, Seungjin Choi, and Yee Whye Teh. 2019. Set Transformer: A Framework for Attention-based Permutation-Invariant Neural Networks. In *Proceedings of the 36th International Conference on Machine Learning (Proceedings of Machine Learning Research, Vol. 97)*, Kamalika Chaudhuri and Ruslan Salakhutdinov (Eds.). PMLR, 3744–3753. <https://proceedings.mlr.press/v97/lee19d.html>
- [71] Yoonho Lee and Seungjin Choi. 2018. Gradient-based meta-learning with learned layerwise metric and subspace. In *International Conference on Machine Learning*. PMLR, 2927–2936.
- [72] Dongxu Li, Junnan Li, Hung Le, Guangsen Wang, Silvio Savarese, and Steven C.H. Hoi. 2023. LAVIS: A One-stop Library for Language-Vision Intelligence. In *Proceedings of the 61st Annual Meeting of the Association for Computational Linguistics (Volume 3: System Demonstrations)*. Association for Computational Linguistics, Toronto, Canada, 31–41. <https://aclanthology.org/2023.acl-demo.3>
- [73] Junnan Li, Dongxu Li, Silvio Savarese, and Steven Hoi. 2023. Blip-2: Bootstrapping language-image pre-training with frozen image encoders and large language models. In *International conference on machine learning*. PMLR, 19730–19742.
- [74] Junnan Li, Dongxu Li, Caiming Xiong, and Steven Hoi. 2022. Blip: Bootstrapping language-image pre-training for unified vision-language understanding and generation. In *International conference on machine learning*. PMLR, 12888–12900.
- [75] Kyungsun Lim, Nyeong-Ho Shin, Young-Yoon Lee, and Chang-Su Kim. 2020. Order Learning and Its Application to Age Estimation. In *International Conference on Learning Representations*. <https://openreview.net/forum?id=HygsuaNFwr>
- [76] Lu Liu, Nima Dehghan, Jillian Chown, C. Giles, and Dashun Wang. 2021. Understanding the onset of hot streaks across artistic, cultural, and scientific careers. *Nature Communications* 12 (09 2021).
- [77] Lu Liu, Yang Wang, Roberta Sinatra, C. Giles, Chaoming Song, and Dashun Wang. 2018. Hot streaks in artistic, cultural, and scientific careers. *Nature* 559 (07 2018).
- [78] Xiaofeng Liu, Zhenhua Guo, Site Li, Ping Jia, Lingsheng Kong, Jane You, and B. V. K. Vijaya Kumar. 2019. Permutation-Invariant Feature Restructuring for Correlation-Aware Image Set-Based Recognition. In *2019 IEEE/CVF International Conference on Computer Vision (ICCV)*. 4985–4995. doi:10.1109/ICCV.2019.00509
- [79] Yinhan Liu, Myle Ott, Naman Goyal, Jingfei Du, Mandar Joshi, Danqi Chen, Omer Levy, Mike Lewis, Luke Zettlemoyer, and Veselin Stoyanov. 2019. RoBERTa: A Robustly Optimized BERT Pretraining Approach. *arXiv preprint arXiv:1907.11692* (2019).
- [80] Zhuang Liu, Hanzi Mao, Chao-Yuan Wu, Christoph Feichtenhofer, Trevor Darrell, and Saining Xie. 2022. A ConvNet for the 2020s. In *2022 IEEE/CVF Conference on Computer Vision and Pattern Recognition (CVPR)*. 11966–11976. doi:10.1109/CVPR52688.2022.01167
- [81] Lajanugen Logeswaran, Honglak Lee, and Dragomir Radev. 2018. Sentence ordering and coherence modeling using recurrent neural networks. In *Proceedings of the Thirty-Second AAAI Conference on Artificial Intelligence and Thirtieth*

- Innovative Applications of Artificial Intelligence Conference and Eighth AAAI Symposium on Educational Advances in Artificial Intelligence* (New Orleans, Louisiana, USA) (AAAI'18/AAAI'18/EAAT'18). AAAI Press, Article 648, 3308 pages.
- [82] Ilya Loshchilov and Frank Hutter. 2017. SGDR: Stochastic Gradient Descent with Warm Restarts. In *International Conference on Learning Representations (ICLR)*.
- [83] Hui Mao, Ming Cheung, and James She. 2017. DeepArt: Learning Joint Representations of Visual Arts. In *Proceedings of the 25th ACM International Conference on Multimedia* (Mountain View, California, USA) (MM '17). Association for Computing Machinery, New York, NY, USA, 1183–1191. doi:10.1145/3123266.3123405
- [84] Oded Maron and Tomás Lozano-Pérez. 1997. A Framework for Multiple-Instance Learning. In *Advances in Neural Information Processing Systems*, M. Jordan, M. Kearns, and S.olla (Eds.), Vol. 10. MIT Press. https://proceedings.neurips.cc/paper_files/paper/1997/file/82965d4ed8150294d4330ace00821d77-Paper.pdf
- [85] Matthias Mauch, Robert M. MacCallum, Mark Levy, and Armand M. Leroi. 2015. The evolution of popular music: USA 1960–2010. *Royal Society Open Science* 2, 5 (2015), 150081. doi:10.1098/rsos.150081 arXiv:<https://royalsocietypublishing.org/doi/pdf/10.1098/rsos.150081>
- [86] David Meredith (Ed.). 2016. *Computational Music Analysis* (1 ed.). Springer, Germany. doi:10.1007/978-3-319-25931-4
- [87] MetPublications. [n. d.]. MetPublications is an online portal to The Metropolitan Museum of Art's comprehensive art publishing program. <https://www.metmuseum.org/met-publications/>
- [88] Jean-Baptiste Michel, Yuan Kui Shen, Aviva Presser Aiden, Adrian Veres, Matthew K. Gray, The Google Books Team, Joseph P. Pickett, Dale Hoiberg, Dan Clancy, Peter Norvig, Jon Orwant, Steven Pinker, Martin A. Nowak, and Erez Lieberman Aiden. 2011. Quantitative Analysis of Culture Using Millions of Digitized Books. *Science* 331, 6014 (2011), 176–182. doi:10.1126/science.1199644 arXiv:<https://www.science.org/doi/pdf/10.1126/science.1199644>
- [89] Youssef Mohamed, Faizan Farooq Khan, Kilicbek Haydarov, and Mohamed Elhoseiny. 2022. It is Okay to Not Be Okay: Overcoming Emotional Bias in Affective Image Captioning by Contrastive Data Collection. In *2022 IEEE/CVF Conference on Computer Vision and Pattern Recognition (CVPR)*. 21231–21240. doi:10.1109/CVPR52688.2022.02058
- [90] Kana Moriwaki, Takahiro Nishimichi, and Naoki Yoshida. 2023. Machine learning for observational cosmology. *Reports on Progress in Physics* 86, 7 (may 2023), 076901. doi:10.1088/1361-6633/acd2ea
- [91] Joaquín Muñoz Sabater, Emanuel Dutra, Anna Agusti-Panareda, Clement Albergel, Gabriele Arduini, Gianpaolo Balsamo, Souhail Boussetta, Margarita Chouga, Shaun Harrigan, Hans Hersbach, Brecht Martens, Diego Miralles, Maria Piles, Nemesio Rodriguez-Fernandez, Ervin Zsótér, Carlo Buontempo, and J.-N. Thépaut. 2021. ERA5-Land: a state-of-the-art global reanalysis dataset for land applications. *Earth System Science Data* 13 (09 2021), 4349–4383. doi:10.5194/essd-13-4349-2021
- [92] R. Myneni, Shabanov N., Yuri Knyazikhin, Wenze Yang, Dong Huang, and Bin Tan. 2002. MOD15A2: Global LAI and FPAR. *AGU Fall Meeting Abstracts* (12 2002).
- [93] Zhenxing Niu, Mo Zhou, Le Wang, Xinbo Gao, and Gang Hua. 2016. Ordinal regression with multiple output cnn for age estimation. In *Proceedings of the IEEE conference on computer vision and pattern recognition*. 4920–4928.
- [94] Samuel E. L. Oliveira, Victor Diniz, Anisio Lacerda, Luiz Merschmann, and Gisele L. Pappa. 2020. Is Rank Aggregation Effective in Recommender Systems? An Experimental Analysis. *ACM Trans. Intell. Syst. Technol.* 11, 2, Article 16 (jan 2020), 26 pages. doi:10.1145/3365375
- [95] Gwenolé Quellec, Guy Cazuguel, Béatrice Cochener, and Mathieu Lamard. 2017. Multiple-Instance Learning for Medical Image and Video Analysis. *IEEE Reviews in Biomedical Engineering* 10 (2017), 213–234. doi:10.1109/RBME.2017.2651164
- [96] Alec Radford, Jong Wook Kim, Chris Hallacy, Aditya Ramesh, Gabriel Goh, Sandhini Agarwal, Girish Sastry, Amanda Askell, Pamela Mishkin, Jack Clark, et al. 2021. Learning transferable visual models from natural language supervision. In *International conference on machine learning*. PMLR, 8748–8763.
- [97] Siamak Ravanbakhsh, Junier Oliva, Sebastien Fromenteau, Layne C. Price, Shirley Ho, Jeff Schneider, and Barnabás Póczos. 2016. Estimating cosmological parameters from the dark matter distribution. In *Proceedings of the 33rd International Conference on International Conference on Machine Learning - Volume 48* (New York, NY, USA) (ICML '16). JMLR.org, 2407–2416.
- [98] Aadirupa Saha, Tomer Koren, and Yishay Mansour. 2021. Adversarial Dueling Bandits. In *Proceedings of the 38th International Conference on Machine Learning (Proceedings of Machine Learning Research, Vol. 139)*, Marina Meila and Tong Zhang (Eds.). PMLR, 9235–9244.
- [99] M. Schuster and K.K. Paliwal. 1997. Bidirectional recurrent neural networks. *IEEE Transactions on Signal Processing* 45, 11 (1997), 2673–2681. doi:10.1109/78.650093
- [100] Stoyan V. Spoure, Erik Aadland, and Giovanni Formilan. 2023. Relations in Aesthetic Space: How Color Enables Market Positioning. *Administrative Science Quarterly* 68, 1 (2023), 146–185. doi:10.1177/00018392221137289 arXiv:<https://doi.org/10.1177/00018392221137289>
- [101] Faisal Shafait and Ray Smith. 2010. Table detection in heterogeneous documents. In *Document Analysis Systems (2010-07-07) (ACM International Conference Proceeding Series)*, David S. Doermann, Venu Govindaraju, Daniel P. Lopresti, and Premkumar Natarajan (Eds.). ACM, 65–72. <http://dblp.uni-trier.de/db/conf/das/das2010.html#ShafaitS10>
- [102] Dean Keith Simonton. 1999. *Origins of genius: Darwinian perspectives on creativity*. Oxford University Press.
- [103] K Simonyan and A Zisserman. 2015. Very deep convolutional networks for large-scale image recognition. *3rd International Conference on Learning Representations (ICLR 2015)*, 1–14.
- [104] Samridhhi Singla, Ayan Mukhopadhyay, Michael Wilbur, Tina Diao, Vinayak Gajjewar, Ahmed Eldawy, Mykel J Kochenderfer, Ross Shachter, and Abhishek Dubey. 2021. WildfireDB: An Open-Source Dataset Connecting Wildfire Occurrence with Relevant Determinants. In *Proceedings of the Neural Information Processing Systems Track on Datasets and Benchmarks*, J. Vanschoren and S. Yeung (Eds.), Vol. 1. https://datasets-benchmarks-proceedings.neurips.cc/paper_files/paper/2021/file/3fe94a002317b5f9259f82690ae4c4d-Paper-round2.pdf
- [105] Konstantinos Skianis, Giannis Nikolentzos, Stratis Limnios, and Michalis Vazirgiannis. 2020. Rep the Set: Neural Networks for Learning Set Representations. In *Proceedings of the 23rd International Conference on Artificial Intelligence and Statistics*. 1410–1420.
- [106] Jake Snell, Kevin Swersky, and Richard Zemel. 2017. Prototypical Networks for Few-shot Learning. In *Advances in Neural Information Processing Systems*, I. Guyon, U. Von Luxburg, S. Bengio, H. Wallach, R. Fergus, S. Vishwanathan, and R. Garnett (Eds.), Vol. 30. Curran Associates, Inc. https://proceedings.neurips.cc/paper_files/paper/2017/file/cb8da6767461f2812ae4290eac7cbc42-Paper.pdf
- [107] Gjorgji Strezoski and Marcel Worring. 2018. OmniArt: A Large-Scale Artistic Benchmark. *ACM Trans. Multimedia Comput. Commun. Appl.* 14, 4, Article 88 (Oct. 2018), 21 pages. doi:10.1145/3273022
- [108] Zhiqing Sun, Jian Tang, Pan Du, Zhihong Deng, and Jian-Yun Nie. 2019. DivGraphPointer: A Graph Pointer Network for Extracting Diverse Keyphrases. *Proceedings of the 42nd International ACM SIGIR Conference on Research and Development in Information Retrieval* (2019). <https://api.semanticscholar.org/CorpusID:159040867>
- [109] Peter Sunehag, Guy Lever, Audrunas Gruslys, Wojciech Marian Czarnecki, Vinicius Zambaldi, Max Jaderberg, Marc Lanctot, Nicolas Sonnerat, Joel Z. Leibo, Karl Tuyls, and Thore Graepel. 2018. Value-Decomposition Networks For Cooperative Multi-Agent Learning Based On Team Reward. In *Proceedings of the 17th International Conference on Autonomous Agents and MultiAgent Systems* (Stockholm, Sweden) (AAMAS '18). International Foundation for Autonomous Agents and Multiagent Systems, Richland, SC, 2085–2087.
- [110] Ilya Sutskever, Oriol Vinyals, and Quoc V. Le. 2014. Sequence to sequence learning with neural networks. In *Proceedings of the 27th International Conference on Neural Information Processing Systems - Volume 2* (Montreal, Canada) (NIPS'14). MIT Press, Cambridge, MA, USA, 3104–3112.
- [111] Wei Ren Tan, Chee Seng Chan, Hernán E Aguirre, and Kiyoshi Tanaka. 2016. Ceci n'est pas une pipe: A deep convolutional network for fine-art paintings classification. In *2016 IEEE international conference on image processing (ICIP)*. IEEE, 3703–3707.
- [112] Yeming Tang and Qiuli Tong. 2016. BordaRank: A ranking aggregation based approach to collaborative filtering. In *2016 IEEE/ACIS 15th International Conference on Computer and Information Science (ICIS)*. 1–6. doi:10.1109/ICIS.2016.7550761
- [113] Andrew J Tatem. 2017. WorldPop, open data for spatial demography. *Scientific data* 4, 1 (2017), 1–4.
- [114] The New York Times. [n. d.]. The New York Times - Breaking News, US News, World News and Videos. <https://www.nytimes.com/>
- [115] H. Tilaver, M. Salti, O. Aydogdu, and E.E. Kungal. 2021. Deep learning approach to Hubble parameter. *Computer Physics Communications* 261 (2021), 107809. doi:10.1016/j.cpc.2020.107809
- [116] Ted Underwood. 2019. *Distant Horizons: Digital Evidence and Literary Change*. University of Chicago Press. doi:10.7208/chicago/9780226612973.001.0001
- [117] Bram van den Akker, Ilya Markov, and Maarten de Rijke. 2019. ViTOR: Learning to Rank Webpages Based on Visual Features. In *The World Wide Web Conference (San Francisco, CA, USA) (WWW '19)*. Association for Computing Machinery, New York, NY, USA, 3279–3285. doi:10.1145/3308558.3313419
- [118] Ashish Vaswani, Noam Shazeer, Niki Parmar, Jakob Uszkoreit, Llion Jones, Aidan N Gomez, Łukasz Kaiser, and Illia Polosukhin. 2017. Attention is All you Need. In *Advances in Neural Information Processing Systems*, I. Guyon, U. Von Luxburg, S. Bengio, H. Wallach, R. Fergus, S. Vishwanathan, and R. Garnett (Eds.), Vol. 30. Curran Associates, Inc. https://proceedings.neurips.cc/paper_files/paper/2017/file/3f5ee243547dee91fdb053c1c4a845aa-Paper.pdf
- [119] Oriol Vinyals, Samy Bengio, and Manjunath Kudlur. 2016. Order matters: Sequence to sequence for sets. In *4th International Conference on Learning Representations, ICLR 2016 - Conference Track Proceedings*. 1–11.
- [120] Oriol Vinyals, Charles Blundell, Timothy Lillicrap, koray kavukcuoglu, and Daan Wierstra. 2016. Matching Networks for One Shot Learning. In *Advances in Neural Information Processing Systems*, D. Lee, M. Sugiyama, U. Luxburg, I. Guyon, and R. Garnett (Eds.), Vol. 29. Curran Associates, Inc. https://proceedings.neurips.cc/paper_files/paper/2016/file/90e1357833654983612fb05e3ec9148c-Paper.pdf
- [121] Z. Wan, S. Hook, and G. Hulley. 2015. MOD11A1 MODIS/Terra Land Surface Temperature/Emissivity Daily L3 Global 1km SIN Grid V006 [Data set]. doi:10.5067/MODIS/MOD11A1.006 Accessed 2024-11-21.

- [122] Jiangliu Wang, Jianbo Jiao, and Yun-Hui Liu. 2020. Self-supervised Video Representation Learning by Pace Prediction. In *Computer Vision – ECCV 2020: 16th European Conference, Glasgow, UK, August 23–28, 2020, Proceedings, Part XVII* (Glasgow, United Kingdom). Springer-Verlag, Berlin, Heidelberg, 504–521. doi:10.1007/978-3-030-58520-4_30
- [123] Tianming Wang and Xiaojun Wan. 2019. Hierarchical attention networks for sentence ordering. In *Proceedings of the Thirty-Third AAAI Conference on Artificial Intelligence and Thirty-First Innovative Applications of Artificial Intelligence Conference and Ninth AAAI Symposium on Educational Advances in Artificial Intelligence* (Honolulu, Hawaii, USA) (AAAI’19/IAAI’19/EAAI’19). AAAI Press, Article 882, 1008 pages. doi:10.1609/aaai.v33i01.33017184
- [124] Yu-An Wang and Yun-Nung Chen. 2020. What Do Position Embeddings Learn? An Empirical Study of Pre-Trained Language Model Positional Encoding. In *Proceedings of the 2020 Conference on Empirical Methods in Natural Language Processing (EMNLP)*, Bonnie Webber, Trevor Cohn, Yulan He, and Yang Liu (Eds.). Association for Computational Linguistics, Online, 6840–6849. doi:10.18653/v1/2020.emnlp-main.555
- [125] Nachoem M. Wijnberg and Gerda Gemser. 2000. Adding Value to Innovation: Impressionism and the Transformation of the Selection System in Visual Arts. *Organization Science* 11, 3 (2000), 323–329. <http://www.jstor.org/stable/2640265>
- [126] WikiArt. [n. d.]. Visual Art Encyclopedia. <https://www.wikiart.org/>
- [127] Wikipedia. [n. d.]. Wikipedia, the free encyclopedia. <https://www.wikipedia.org/>
- [128] Michael J. Wilber, Chen Fang, Hailin Jin, Aaron Hertzmann, John Collomosse, and Serge Belongie. 2017. BAM! The Behance Artistic Media Dataset for Recognition Beyond Photography. In *The IEEE International Conference on Computer Vision (ICCV)*.
- [129] Karen Wilkin. 1993. After the Retrospective: Matisse and Picasso. *The Hudson Review* 46, 1 (1993), 195–200. <http://www.jstor.org/stable/3852316>
- [130] Oliver E Williams, Lucas Lacasa, and Vito Latora. 2019. Quantifying and predicting success in show business. *Nature communications* 10, 1 (2019), 1–8.
- [131] Zhirong Wu, Shuran Song, Aditya Khosla, Fisher Yu, Linguang Zhang, Xiaoou Tang, and Jianxiong Xiao. 2015. 3D ShapeNets: A deep representation for volumetric shapes. In *2015 IEEE Conference on Computer Vision and Pattern Recognition (CVPR)*, 1912–1920. doi:10.1109/CVPR.2015.7298801
- [132] Wenju Xu, Chengjiang Long, and Yongwei Nie. 2023. Learning Dynamic Style Kernels for Artistic Style Transfer. In *Proceedings of the IEEE/CVF Conference on Computer Vision and Pattern Recognition (CVPR)*, 10083–10092.
- [133] Yuji Yamamoto and Takuya Matsuzaki. 2023. Absolute Position Embedding Learns Sinusoid-like Waves for Attention Based on Relative Position. In *The 2023 Conference on Empirical Methods in Natural Language Processing*. <https://openreview.net/forum?id=zpayaLaUHL>
- [134] Le Yan, Zhen Qin, Xuanhui Wang, Gil Shamir, and Mike Bendersky. 2023. Learning to Rank when Grades Matter. *arXiv preprint arXiv:2306.08650* (2023).
- [135] X. Yang, B. Gao, C. Xing, Z. Huo, X. Wei, Y. Zhou, J. Wu, and X. Geng. 2015. Deep Label Distribution Learning for Apparent Age Estimation. In *2015 IEEE International Conference on Computer Vision Workshop (ICCVW)*, 344–350. doi:10.1109/ICCVW.2015.53
- [136] Tetiana Yemelianenko, Iuliia Tkachenko, Tess Masclef, Mihaela Scuturici, and Serge Miguet. 2023. Learning to Rank Approach for Refining Image Retrieval in Visual Arts. In *Proceedings of the IEEE/CVF International Conference on Computer Vision (ICCV) Workshops*, 1623–1631.
- [137] Nikolaos-Antonios Ypsilantis, Noa Garcia, Guangxing Han, Sarah Ibrahim, Nanne Van Noord, and Giorgos Toliás. 2021. The Met Dataset: Instance-level Recognition for Artworks. In *Thirty-fifth Conference on Neural Information Processing Systems Datasets and Benchmarks Track (Round 2)*. <https://openreview.net/forum?id=fnuAjFL7MXy>
- [138] Manzil Zaheer, Satwik Kottur, Siamak Ravanbakhsh, Barnabas Poczos, Russ R Salakhutdinov, and Alexander J Smola. 2017. Deep Sets. In *Advances in Neural Information Processing Systems*, I. Guyon, U. Von Luxburg, S. Bengio, H. Wallach, R. Fergus, S. Vishwanathan, and R. Garnett (Eds.), Vol. 30. Curran Associates, Inc. https://proceedings.neurips.cc/paper_files/paper/2017/file/f22e4747da1aa27e363d86d40ff442fe-Paper.pdf
- [139] Lily Zhang, Veronica Tozzo, John Higgins, and Rajesh Ranganath. 2022. Set Norm and Equivariant Skip Connections: Putting the Deep in Deep Sets. In *Proceedings of the 39th International Conference on Machine Learning (Proceedings of Machine Learning Research, Vol. 162)*, Kamalika Chaudhuri, Stefanie Jegelka, Le Song, Csaba Szepesvari, Gang Niu, and Sivan Sabato (Eds.). PMLR, 26559–26574. <https://proceedings.mlr.press/v162/zhang22ac.html>

Supplementary Material

In this supplementary material, we provide additional details to complement the main paper. In Section A, we present the formulas for the training objectives and evaluation metrics used. In Section B, we provide implementation details and visualizations of the static and temporal-aware baseline methods. In Section C, we describe the creation process of the WikiArt-Seq2Rank dataset in detail and include additional results. In Section D, we present a detailed overview of the input variables and temporal embeddings used for the short-term wildfire danger task, along with ablation studies and additional results. Finally, in Section E, we discuss the limitations of this work and its broader impact. To support reproducibility, we plan to release all datasets and model implementations used in this work on GitHub.

A Loss Functions and Evaluation Metrics

In this section, we provide formulas for the training objectives and evaluation metrics.

A.1 Loss Functions

We present the formulas for training our methods for the WikiArt-Seq2Rank predicting artistic success, and the Mesogeos short-term wildfire danger forecasting tasks.

Pointwise Learning-to-Rank. For the WikiArt-Seq2Rank predicting artistic success task, we are adopting the pointwise learning-to-rank approach, and we optimize our methods using the Mean Squared Error (MSE) loss function:

$$MSE(Y, \hat{Y}) = -\frac{1}{K} \sum_{k=1}^K (y_k - \hat{y}_k)^2, \quad (8)$$

where Y denotes the target output, \hat{Y} the predicted output, K denotes the total number of the samples within a batch, y_k the ground-truth label for the sample k , and \hat{y}_k the predicted output for the sample k . For all rankings, we scale the outputs to the $[0,1]$ range.

Cross-Entropy Loss. For the Mesogeos [66] short-term wildfire danger forecasting task, we treat the problem as a binary classification task with two output logits, one for each class. To train the models, we optimize a weighted Cross-Entropy (CE) loss, designed to emphasize larger wildfires while maintaining adequate attention to low-danger instances. The CE loss is defined as:

$$CE(Y, \hat{Y}) = -\frac{1}{K} \sum_{k=1}^K w_k \log \hat{y}_{k, y_k}, \quad (9)$$

where Y denotes the target labels, \hat{Y} the predicted probabilities obtained after applying the log-softmax function to the model’s output logits, K the total number of samples within a batch, $y_k \in \{0,1\}$ the ground-truth label for sample k , and \hat{y}_{k, y_k} the predicted probability for the correct class y_k for sample k .

Following the same approach as in [66], the weight w_k for each sample is calculated based on the burned area size of the corresponding wildfire. To ensure the model learns to assign greater danger to larger fires, the Cross-Entropy loss is multiplied by the logarithmic transformation of the burned area size:

$$w_k = \begin{cases} \log(\text{burned_area}_k + 1), & \text{if } y_k = 1, \\ \min(\log(\text{burned_area}_p + 1)), & \text{if } y_k = 0, \end{cases} \quad (10)$$

where burned_area_k is the burned area size for sample k , and $\min(\log(\text{burned_area}_p + 1))$ represents the minimum weight assigned to positive samples. This ensures that low-danger negative samples receive sufficient attention during training. The logarithmic transformation of the burned area size mitigates the risk of larger fires dominating the learning process by narrowing the penalization gap between small and large fires, as described in [66].

A.2 Evaluation Metrics

Here, we detail the evaluation metrics for the WikiArt-Seq2Rank predicting artistic success, and the Mesogeos short-term wildfire danger forecasting tasks.

Evaluation metrics for predicting artistic success. During inference, we process each artist individually by setting the batch size equal to 1 to alleviate issues arising from the varying size of sets and length of sequences. Inspired by research in information ordering [11, 68, 69, 81, 123], we report Kendall’s τ [64] and Mean Absolute Error (MAE) [135] to evaluate the performance of the proposed methods. *Kendall’s τ .* We compute Kendall’s τ as follows:

$$\tau(Y, \hat{Y}) = 1 - \frac{2(\# \text{ inversions})}{K(K-1)/2}, \quad (11)$$

where K denotes the total number of samples and $\#$ number of inversions of consecutive items in the predicted ranking \hat{Y} necessary to arrange them to match the target ranking Y .

Mean Absolute Error (MAE). We compute the Mean Absolute Error (MAE) as follows:

$$MAE(Y, \hat{Y}) = -\frac{1}{K} \sum_{k=1}^K |y_k - \hat{y}_k|, \quad (12)$$

where Y denotes the ground-truth and \hat{Y} the predicted ranking as in Eq. (8).

Evaluation metrics for short-term wildfire danger forecasting. Following [66], we report the F1-score and Precision-Recall Area Under the Curve (PR-AUC) to evaluate the performance of the proposed methods.

F1-score. The F1-score provides a balance between precision and recall, capturing overall performance in binary classification tasks. It is computed as follows:

$$F1\text{-score} = 2 \cdot \frac{\text{Precision} \cdot \text{Recall}}{\text{Precision} + \text{Recall}}, \quad (13)$$

where Precision is defined as:

$$\text{Precision} = \frac{\text{True Positives}}{\text{True Positives} + \text{False Positives}}, \quad (14)$$

and Recall is defined as:

$$\text{Recall} = \frac{\text{True Positives}}{\text{True Positives} + \text{False Negatives}}. \quad (15)$$

Precision-Recall Area Under the Curve (PR-AUC). The PR-AUC measures the relationship between precision and recall across varying

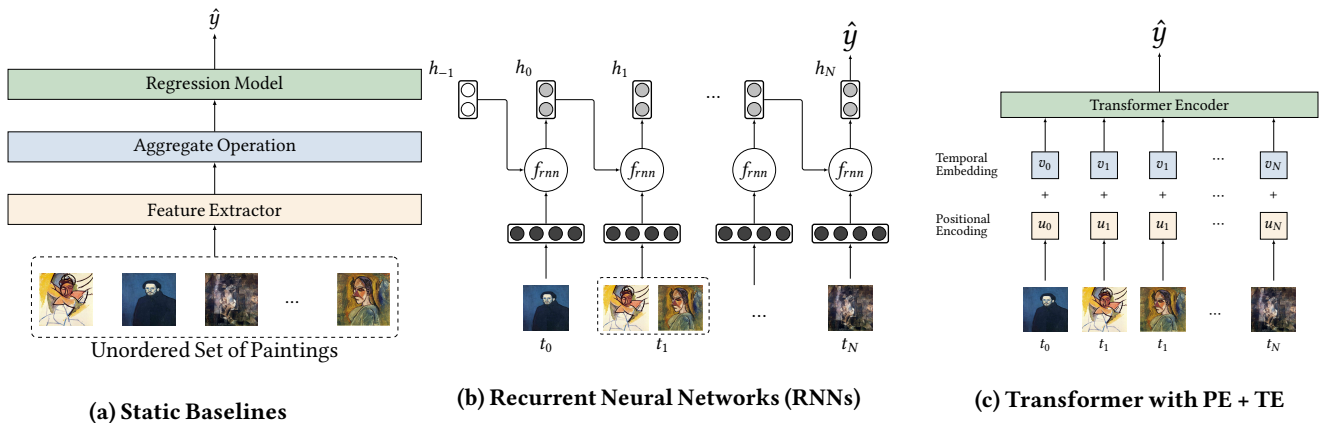


Figure 4: Visualization of three different static and temporal-aware baselines. \hat{y} denotes the predicted output. (a) **Static Baselines** illustrates the procedure of our static baselines. Given an unordered set \mathcal{S} , first we extract representations of the instances x_i in the set \mathcal{S} , thereafter we aggregate them utilizing a merging operation and finally we feed the representation forward to a regression or classification model. (b) **Recurrent Neural Networks (RNNs)** illustrates the procedure of the RNN-based baselines. Given an ordered input sequence \mathcal{T} , we aggregate the instances within a set \mathcal{S} at timestep t_i and we feed the sequential-structured representations forward to an RNN-based temporal-aware baseline. (c) **Transformer with Positional Encoding (PE) and Temporal Embedding (TE)** illustrates the procedure of the Transformer-based baselines. Given an ordered input sequence \mathcal{T} , we first extract representations of the different instances within a set \mathcal{S} at timestep t_i , and thereafter we combine them with the positional encoding and temporal embedding of timestep t_i . Finally, we feed the obtained representation forward to a Transformer encoder module.

thresholds. It is defined as:

$$PR-AUC = \int_0^1 \text{Precision}(\text{Recall})d(\text{Recall}), \quad (16)$$

where $\text{Precision}(\text{Recall})$ represents precision as a function of recall. In practice, this integral is approximated as:

$$PR-AUC = \sum_{i=1}^{N-1} (\text{Recall}_{i+1} - \text{Recall}_i) \cdot \text{AvgPrecision}_i, \quad (17)$$

with AvgPrecision_i as the average precision at successive recall thresholds.

B Static and Temporal-Aware Baselines

Figure 4 illustrates three static and temporal-aware baseline methods considered in this work.

Static baselines. Figure 4(a) illustrates the procedure of our static baselines. First, we extract feature vectors to represent each instance x_i for a set \mathcal{S} of unordered instances x_i . We aggregate the feature vectors of all instances in \mathcal{S} to obtain its representation. Finally, we use a regression or classification model to obtain the predicted output \hat{y} for the set \mathcal{S} . Note that for the WikiArt-Seq2Rank task, for our static baselines each artist in our corpus correspond to one unordered set \mathcal{S} of visual instances. We consider the following static baselines:

- **Vanilla:** For the WikiArt-Seq2Rank task, we use a plain linear regression-based method that uses simple aggregation operations over all the available instances, artworks, associated to a focal artist to obtain its representation.
- **Gradient Boosting [24]:** For the WikiArt-Seq2Rank task, we use a Gradient Boosting an ensemble method with strong performance on different learning-to-rank tasks. Similar to

our Vanilla baseline, we use aggregation operations to obtain an artist representation. For implementation we use the XGBoost library [24].

- **DeepSets [138]:** Static DeepSets employing mean and max aggregation operations as described in Section 3 of the main paper, and adding a final fully connected-layer to obtain the final output. For DeepSets, we are using the implementation provided in [70].
- **Set Transformer [70]:** Static Set Transformer using three different variants as described in Section 3 of the main paper, using the implementation provided in [70]. For each variant, we add a final fully connected-layer to obtain the final output.

Temporal-aware baselines. Figure 4(b-c) illustrates the procedure of two temporal-aware baseline methods.

Recurrent Neural Networks (RNNs). Figure 4(b) illustrates the procedure of our temporal-aware RNN-based baseline. Given an ordered input sequence of sets \mathcal{S} , we first aggregate the feature vectors of instances observed at the same timestep t_i to obtain a set representation s_i for the timestep t_i . Thereafter, we feed the sequential-structured representations forward to an RNN-based module. In this work, we utilize Long Short Term Memory networks (LSTMs) [53] as our RNN-based module. Specifically, we employ a bidirectional LSTM coupled with attention-mechanism as described in Section 4 of the main paper.

Transformer. Figure 4(c) illustrates the procedure of our temporal-aware Transformer-based baseline. Given an ordered input sequence of sets \mathcal{S} , we first extract the feature vector representations x_i of the instances observed at a timestep t_i . We combine the feature vector representations for each instance at timestep t_i with the positional encoding u_i and temporal embedding v_i of timestep t_i . Finally, the

obtained representation, i.e., the sum of the feature vector s_i , positional encoding u_i and temporal embedding v_i is fed forward to a Transformer encoder. In this work, we utilize a Transformer encoder module [118] as described in Section 4 of the main paper.

For our temporal-based baselines, we consider the following:

- HierarchicalDeepSets: An extension of DeepSets for temporal-aware learning of set representations, i.e., we learn a set representation for each timestep t_i for an ordered sequence \mathcal{T} , and a set representation for the sequence \mathcal{T} .
- BiLSTM + ATTN: A bidirectional LSTM [53] method coupled with attention mechanism [7] that learns sequential representations over aggregates of sets. We use two stacked layers and set the hidden dimensionality to 512.
- Transformer: A Transformer encoder module [118] as described in Section 3 of the main paper with the modification of flattening the temporal representations over the sequence of sets, i.e., all instances in the set s_0 at timestep t_0 have a 0-th indexed positional encoding and a 0-th indexed temporal embedding, but their own representation x_{0j} as obtained from Eq. (2) of the main paper.

C WikiArt-Seq2Rank

Here, we describe in full detail how our WikiArt-Seq2Rank dataset was created.

C.1 Dataset Statistics

We make use of the WikiArt collection [126] that has been extensively studied in automatic fine-art analysis [2, 19, 39, 40, 89, 111, 136]. Following [39, 40], we use the publicly available version of the WikiArt dataset that consists of 75,921 paintings created by 1,111 artists from 1401 up to 2012, spanning 20 stylistic movements ranging from *Early Renaissance* to *Contemporary Art*. We omit artworks without a known creation date and artists that have less than 10 artworks in the collection. This results in a dataset that consists of 59,458 artworks, created by 849 artists. The curated dataset provides also annotations based on 4,513 unique tags associated with the 59,458 artworks. In addition, it contains annotations of the most popular artworks for different artists as provided in the WikiArt collection, 4,711 artworks in total. Note that in this work we only model the visual content and the creation period associated with the different artworks. Table 3 summarizes the statistics of the WikiArt-Seq2Rank dataset. We extend the publicly available WikiArt dataset using additional information provided from various sources to construct rankings based on artist appreciation for the 849 artists in our dataset.

C.2 Rankings Construction

We considered several sources to construct our artist appreciation rankings according to various audiences. Following previous work in rank aggregation [6, 38, 94, 112], we use the Borda count system [30] to aggregate different rankings when necessary. In this work, we consider the following rankings:

eBooks. We gathered 904 art-related digitized books, eBooks, from four different sources. For each source, we collected eBooks in Portable Document Format (PDF). We proceed by using Optical Character Recognition (OCR) to convert any scanned eBooks to editable format using Tesseract [101]. For each eBook, we perform

Table 3: Statistics of the WikiArt-Seq2Rank dataset.

Property	Max/Average/Total(#)
#Artists	849
#Paintings	59,458
Time Period	1409 - 2012
Max paintings/artist	1,884
Average paintings/artist	70.03
Max sequences/artist	77
Average sequences/artist	18.87
Max paintings/timestep	326
Average paintings/timestep	5.06
#Rankings	10

Named Entity Recognition (NER) using the spaCy [54] implementation of RoBERTa [79] and we keep all named entities that belong to the specific label “PERSON”. Finally, we count the number of eBooks that any of the artists in our corpus are mentioned in, and rank the artists accordingly.

The Met Collection. We collected 601 digitized eBooks from the Met-Publications publicly available service [87]. For this source, 47% (396 out of 894) of the artists in our corpus have at least one mention in any of the 601 available eBooks.

The Guggenheim Collection. We collected 192 digitized eBooks from the Guggenheim Publications publicly available service [50]. For this source, 40% (341 out of 894) of the artists in our corpus have at least one mention in any of the 192 available eBooks.

The Getty Collection. We collected 70 digitized eBooks from the Getty Publications publicly available service [47]. For this source, 32% (270 out of 894) of the artists in our corpus have at least one mention in any of the 70 available eBooks.

University Library. We manually collected 41 art-related eBooks from an online university library. For this source, 30% (251 out of 894) of the artists in our corpus have at least one mention in any of the 41 available eBooks.

Using the Borda count system we create a final aggregate ranking, which we refer to as eBooks. In this ranking, 65% (550 out of 849) of the artists in our dataset are mentioned at least once in any of the available eBooks of the four collections.

The New York Times (NYT). We make use of the publicly available archive¹ of The New York Times [114] and retrieved 4,525 total abstracts of art-related reviews published from 1981–2019. We use the same procedure as in eBooks to extract entities and count the number of times an artist is mentioned in any abstract. In this ranking, 47% (401 out of 849) of the artists in our data have at least one mention in an abstract.

Wikipedia Mentions. We collected all the available pages in the English section of Wikipedia [127] of the artists in our corpus. We use the same procedure as in eBooks and The New York Times rankings to extract entities and count the number of times an artist is mentioned in another artist’s Wikipedia page. This resulted in a

¹<https://developer.nytimes.com/docs/archive-product/1/overview/>

Table 4: Statistics on rankings creation and different splitting strategies for the WikiArt-Seq2Rank dataset. For dataset splits, the number of artists and paintings (inside parentheses) are given. Ranked denotes the number of artists ranked per individual ranking (out of the 849 artists in our corpus). Ties denotes the number of rank positions that consist of more than one artist. Range denotes the minimum and maximum ranked positions (all not-ranked artists are tied in the last position denoted with 1). Time Period denotes the period of time in which the different source provides information regarding the ranked artists. Aggregate denotes the final aggregate operation for constructing a single ranking per source. Time Series Split row represents the number of artists and paintings (in parentheses) for all rankings considered. N/A denotes Not Applicable.

Ranking	Stratified Split			Ranked	Ties	Range	Time Period	Aggregate
	Train	Validation	Test					
eBooks	591 (40,369)	81 (6,647)	177 (12,442)	550	63	[1, 346]	N/A	Borda count on four publicly available sources
The New York Times	591 (37,261)	83 (7,752)	175 (14,445)	401	39	[1, 62]	January, 1981 - December, 2019	Sum over Time
Wikipedia Mentions	590 (40,480)	81 (4,612)	178 (14,366)	732	26	[1, 44]	N/A	Sum
Wikipedia Links	591 (43,030)	82 (4,834)	176 (11,594)	560	30	[1, 40]	N/A	Sum
Wikipedia Pageviews	589 (41,046)	80 (4,830)	180 (13,582)	817	1	[1, 818]	July, 2015 - December, 2020	Sum over Time
Google Ngram	589 (39,819)	80 (4,915)	180 (14,724)	691	1	[1, 692]	16th Century - 21st Century	Sum over Time
Google Trends	591 (42,542)	81 (4,164)	177 (12,752)	554	66	[1, 385]	April, 2017 - April, 2022	Sum over Time
Artfacts	591 (41,155)	81 (7,009)	177 (11,294)	441	2	[1, 441]	January, 2016 - December, 2016	N/A
Artprice	592 (42,122)	82 (5,422)	175 (11,914)	366	18	[1, 349]	January, 2006 - December, 2021	Borda count on the Top-500 annual rankings
Aggregate Ranking	589 (42,439)	80 (6,023)	180 (10,996)	833	26	[1, 809]	N/A	Borda count on all the individual rankings
Time Series Split	601 (51,928)	83 (3,407)	165 (4,123)	N/A	N/A	N/A	N/A	N/A

Table 5: Top-10 artists per ranking. \uparrow denotes ascending order.

eBooks \uparrow	The New York Times \uparrow	Wikipedia Mentions \uparrow	Wikipedia Links \uparrow	Wikipedia Pageviews \uparrow	Google Ngram \uparrow	Google Trends \uparrow	Artfacts \uparrow	Artprice \uparrow	Aggregate Ranking \uparrow
Michelangelo	Andy Warhol	Pablo Picasso	Pablo Picasso	Winston Churchill	Titian	Vincent van Gogh	Andy Warhol	Pablo Picasso	Pablo Picasso
Raphael	Michelangelo	Michelangelo	Henri Matisse	Leonardo da Vinci	Raphael	Pablo Picasso	Pablo Picasso	Andy Warhol	Andy Warhol
Leonardo da Vinci	Roy Lichtenstein	Henri Matisse	Paul Cézanne	Vincent van Gogh	Rembrandt	Salvador Dali	Bruce Nauman	Claude Monet	Vincent van Gogh
Paul Cézanne	John Russell	Raphael	Jackson Pollock	Pablo Picasso	Winston Churchill	Andy Warhol	Gerhard Richter	Gerhard Richter	Jackson Pollock
Pablo Picasso	Willem De Kooning	Titian	Michelangelo	Andy Warhol	Leonardo da Vinci	Leonardo da Vinci	Sol Lewitt	Roy Lichtenstein	Claude Monet
Vincent van Gogh	Richard Serra	Jackson Pollock	Leonardo da Vinci	Michelangelo	Michelangelo	Michelangelo	Man Ray	Marc Chagall	Henri Matisse
Claude Monet	Jackson Pollock	Paul Cézanne	Titian	Salvador Dali	Joshua Reynolds	Claude Monet	Roy Lichtenstein	Joan Miro	Mark Rothko
Rembrandt	David Smith	Rembrandt	Raphael	Claude Monet	Tintoretto	Rembrandt	Marcel Duchamp	Willem De Kooning	Paul Klee
Édouard Manet	Sol Lewitt	Mark Rothko	Mark Rothko	Jackson Pollock	Donatello	Caravaggio	Richard Serra	Alexander Calder	Paul Gauguin
Edgar Degas	Mark Rothko	Georges Braque	Vincent van Gogh	Rembrandt	Le Corbusier	Wassily Kandinsky	Paul Klee	Henri Matisse	Edgar Degas

ranking where 86% (732 out of 849) of the artists are mentioned at least once in another artist’s Wikipedia page.

Wikipedia Links. We use all the available pages in the English section of Wikipedia of the artists in our corpus, and count the number of times an artist’s Wikipedia page uniform resource locator (URL) is linked to another artist’s Wikipedia page. This resulted in a ranking where 66% (560 out of 849) of the artists’ Wikipedia pages are linked to at least another artist’s Wikipedia page.

Wikipedia Pageviews. We use the pageviews statistics² as provided by Wikipedia to create a ranking by collecting artists’ English Wikipedia pages that were accessed by the public between July, 2015 and December, 2020. We create a ranking by aggregating the number of times an artist’s English Wikipedia page was accessed by an individual. This resulted in a ranking where 96% (817 out of 849) of the artists’ Wikipedia pages were accessed at least once.

Google Ngram. We use the Google Books Ngram Viewer [88] on a yearly basis, counting the number of times an artist was mentioned in any book using the American English Google Books corpus (2019 version). This resulted in a ranking where 81% (691 out of 849) of the artists in our corpus are mentioned at least once.

Google Trends. We use the Google Trends service [48]. We utilize the relative frequency of an artist being searched using Google Search for the Google category “Painting” from April 23, 2017, up

to April 23, 2022. We identified 554 artists in our corpus that have a valid Google topic identifier and compared their respective frequency of being searched to the topic “Painter”. This resulted in a ranking where 65% (554 out of 849) of the artists in our corpus were searched from the public using the Google Search service.

Artfacts. We gather artist-specific rankings through Artfacts, a web service [4] that provides art-related rankings based on artists’ exhibitions at museums and art galleries, as provided for the year 2016. This results in a ranking where 52% (441 out of 849) of the artists in our corpus were ranked.

Artprice. We collected publicly available reports from Artprice, a web service that provides information on art auction sales [5]. These reports provide information about the top 500 artists by revenue on a yearly basis from 2006–2021. We use the Borda count system and aggregate the annual rankings. This resulted in a ranking where 43% (366 out of 849) of the artists in our corpus were ranked.

Aggregate Ranking. Further to the individual rankings, we created an overall ranking by aggregating them using the Borda count system [30]. This resulted in a ranking where 98% (833 out of 849) of the artists in our corpus were ranked.

Train/Val/Test splits. We provide two separate settings to evaluate our proposed methods using stratified and times series split strategies. For both settings, each training, validation, and test sample consists of the full career of an artist, either as a static set of multiple

²https://wikimedia.org/api/rest_v1/

Table 6: Results for the predicting artistic success task using the WikiArt-Seq2Rank Time Series Split subset. We report Kendall’s τ and Mean Absolute Error (MAE) for different methods and rankings, as well as overall performance in the Aggregate Ranking and leaderboard scores (BT and Borda). For this setting we omit results with learnable temporal embeddings due to the misalignment of the training and test set. PE denotes the use of positional encodings; (mean) and (max) refer to pooling operations. For Set2Seq Transformer models using Set Transformer only the specific variant is denoted in parentheses. For Kendall’s τ , BT, and Borda, higher (Δ) is better; for MAE, lower (∇) is better. Best results in bold; second best underlined.

Method	Leaderboard		Aggregate Ranking		eBooks		The New York Times		Wikipedia Mentions		Wikipedia Links		Wikipedia Pageviews		Google Ngram		Google Trends		Artfacts		Artprice	
	BT Δ	Borda Δ	$\tau \Delta$	MAE ∇	$\tau \Delta$	MAE ∇	$\tau \Delta$	MAE ∇	$\tau \Delta$	MAE ∇	$\tau \Delta$	MAE ∇	$\tau \Delta$	MAE ∇	$\tau \Delta$	MAE ∇	$\tau \Delta$	MAE ∇	$\tau \Delta$	MAE ∇	$\tau \Delta$	MAE ∇
Vanilla (mean)	1,070	64	0.062	0.960	0.038	1.065	0.013	0.665	0.112	1.123	0.130	1.183	0.026	1.070	0.057	1.161	0.073	1.154	-0.059	1.029	0.021	1.503
Vanilla (max)	1,170	92	0.124	0.571	0.107	0.640	0.154	0.477	0.081	0.299	0.094	0.312	0.051	0.635	0.062	0.792	0.006	0.698	0.118	0.628	0.056	0.672
Gradient Boosting (mean)	1,176	94	0.092	0.264	0.037	0.268	0.105	0.195	-0.052	0.133	0.066	0.152	0.164	0.270	0.079	0.256	-0.038	0.299	0.047	0.314	0.010	0.342
Gradient Boosting (max)	1,414	199	0.222	0.230	0.208	0.213	0.147	0.161	0.018	0.085	0.081	0.094	0.137	0.262	0.074	0.248	0.112	0.231	0.078	0.317	0.154	0.271
DeepSets (mean)	1,346	163	0.136	0.272	0.188	0.153	0.072	0.127	-0.092	0.066	-0.048	0.073	0.139	0.274	0.119	0.240	-0.016	0.132	0.085	0.309	0.024	0.251
DeepSets (max)	1,767	387	0.218	0.216	0.236	0.114	0.171	0.113	0.159	0.051	<u>0.128</u>	0.052	0.197	0.242	<u>0.179</u>	0.219	0.071	0.096	0.100	0.361	0.165	0.185
Set Transformer (SAB + PMA)	1,435	210	0.173	0.232	0.039	0.151	0.111	0.128	0.132	0.063	0.064	0.078	0.134	0.263	0.118	0.247	0.066	0.155	0.112	0.308	0.113	0.260
Set Transformer (ISAB + PMA)	1,465	226	0.105	0.260	0.110	0.121	0.103	0.111	0.052	<u>0.048</u>	0.118	0.052	0.093	0.265	0.063	0.267	0.070	0.115	0.029	0.327	0.162	0.201
Set Transformer (ISAB + PMA + SAB)	1,450	219	0.157	0.232	0.156	0.127	-0.001	0.123	0.023	0.063	0.079	0.075	0.153	0.256	0.170	0.248	0.067	0.146	0.079	0.325	0.143	0.242
Hierarchical DeepSets (max)	1,483	238	0.135	0.264	0.216	0.153	0.087	0.123	0.191	0.065	0.159	0.073	0.182	0.262	0.155	0.244	0.019	0.215	0.129	0.299	0.049	0.305
LSTM (mean)	1,474	232	0.154	0.255	0.192	0.147	0.136	0.122	0.042	0.069	0.089	0.085	0.135	0.256	0.113	0.278	0.169	0.166	0.107	0.315	<u>0.190</u>	0.191
LSTM (max)	1,443	217	0.074	0.279	0.059	0.119	0.083	0.143	0.246	0.057	0.130	0.267	0.107	0.249	0.106	0.257	0.125	0.056	0.317	0.086	0.236	
Transformer w/o PE	1,584	293	0.141	0.250	0.151	0.149	0.143	0.117	0.083	0.058	0.173	0.073	<u>0.223</u>	0.236	0.120	0.286	0.063	<u>0.104</u>	0.119	0.308	0.165	<u>0.185</u>
Transformer + PE	1,600	301	0.178	0.235	0.184	0.172	0.141	0.125	0.088	0.051	0.069	0.062	0.186	0.230	0.136	0.281	0.082	0.119	0.194	0.314	0.193	0.198
Set2Seq BiLSTM (DeepSets - mean)	1,527	261	0.193	0.253	<u>0.240</u>	0.132	0.168	0.115	0.132	0.053	0.108	0.068	0.121	0.250	-0.007	0.245	0.071	0.128	0.102	0.315	0.086	0.247
Set2Seq BiLSTM (DeepSets - max)	1,656	334	0.180	0.239	0.236	0.108	0.241	0.122	<u>0.192</u>	0.052	0.168	0.064	0.189	0.244	0.150	0.254	0.060	0.125	0.111	0.302	0.153	0.269
Set2Seq BiLSTM (SAB + PMA)	1,514	256	0.167	0.240	0.117	0.134	0.132	0.157	0.091	0.076	0.144	0.090	0.183	0.256	0.137	0.246	0.100	0.149	0.110	0.301	0.176	0.231
Set2Seq BiLSTM (ISAB + PMA)	1,476	230	0.157	0.239	0.172	0.140	-0.016	0.124	0.074	0.051	0.160	0.073	0.158	<u>0.234</u>	0.110	0.278	0.094	0.149	0.056	0.335	0.098	0.200
Set2Seq BiLSTM (ISAB + PMA + SAB)	1,445	215	0.127	0.267	0.086	<u>0.109</u>	0.176	0.137	0.125	0.051	0.121	0.071	0.130	0.262	0.080	0.270	0.122	0.187	0.049	0.335	0.100	0.214
Set2Seq Transformer (DeepSets - mean)	1,667	338	<u>0.237</u>	0.225	0.202	0.115	0.184	0.109	0.117	0.049	0.136	0.061	0.195	0.243	0.120	0.265	0.060	0.133	0.145	0.291	0.057	0.214
Set2Seq Transformer (DeepSets - max)	1,786	393	0.236	0.238	0.254	0.125	<u>0.253</u>	0.111	0.170	0.043	0.162	0.055	0.220	0.237	0.205	0.222	0.062	0.111	0.122	0.307	0.104	0.209
Set2Seq Transformer (SAB + PMA)	1,676	344	0.169	0.244	0.174	0.115	0.236	0.119	0.111	0.049	0.166	0.057	0.253	0.236	0.090	0.243	0.104	0.120	0.107	0.294	0.128	0.210
Set2Seq Transformer (ISAB + PMA)	1,618	312	0.221	<u>0.222</u>	0.135	0.131	0.255	0.113	0.095	0.057	0.100	0.069	0.141	0.240	0.100	0.231	0.135	0.113	0.184	0.324	0.069	0.221
Set2Seq Transformer (ISAB + PMA + SAB)	1,758	382	0.259	0.216	0.118	0.110	0.249	0.112	0.127	0.053	0.096	<u>0.054</u>	0.189	0.251	0.147	0.223	0.109	0.128	<u>0.192</u>	0.284	0.160	0.183

instances (artworks) for static methods or as a sequence of sets of multiple instances for sequential methods.

Stratified Split. First, we use a ranking-based stratified split strategy to split the dataset into training (70% of the artists), validation (10% of the artists) and test (20% of the artists) subsets.

Time Series Split. Inspired by real-world applications, in which based on the assessments of known (seen) artists the goal is to predict the artistic performance of unknown (unseen) recently active artists, we split the data at fixed time intervals. We use artists that started their careers before 1930 (exclusive) as the training set (70% of the dataset), the artists that started their careers in the period [1930,1951) as the validation set (10% of the dataset), and the remaining artists that started their careers after the year 1951 (inclusive) as the test set (20% of the dataset).

Table 4 summarizes the statistics for the different rankings and Table 5 provides a list of the top-10 artists per individual ranking.

C.3 Analysis of Learned Representations

In addition to our experimental results, we provide qualitative analysis of our Set2Seq Transformer.

Qualitative analysis of Set2Seq Transformer set and temporal position-aware representations. Inspired by [124], we provide qualitative analysis on the learned position and temporal-aware representations of our Set2Seq Transformer. Figure 6 illustrates the pairwise cosine distances between Pablo Picasso and Andy Warhol for the first ten years of their respective careers, with point at (i, j) illustrating the cosine distance between the i -th horizontal position with the j -th vertical position. An interesting observation based on Figure 6(e), is that the most similar year of Pablo Picasso respective career to Andy Warhol’s is the latest one. In contrast, Andy Warhol’s initial two years are generally closer, especially the second year, to the

first ten years of Pablo Picasso’s career. This is to be expected to a certain degree, given the time difference between the two artists’ careers.

Qualitative analysis on single-instance retrieval. Following [39], we perform qualitative analysis on a paintings retrieval task. In particular, we extract learned representations for DeepSets and Set2Seq Transformer and use k-nearest neighbors (k-NN) to retrieve the top-5 neighbors by cosine distance to a query image. Figure 7 illustrates the results for DeepSets (on the left side) and our Set2Seq Transformer (on the right side). It can be clearly seen that the single-instance DeepSets representations capture some relevant characteristics, while they lack temporal information. In contrast, Set2Seq Transformer representations with position-aware and temporal embeddings retrieve images with similar characteristics, successfully integrating temporal position-aware information with visual content. An interesting observation is that the only misalignment in our Set2Seq Transformer retrieval for Pablo Picasso’s *Les Femmes d’Alger (O. J. R. M.)* is Henri Matisse’s *Landscape with Brook* (1907), an artist with a great influence from and on Pablo Picasso [129].

C.4 Additional Results

Results using the Time Series Split. Table 6 presents the results using the Time Series Split setting. The performance of all methods is degrading when evaluated in our proposed Time Series Split. This is to be expected given this extremely challenging task of predicting the success of modern artists based on historic observations. Nevertheless, it can be easily observed that our Set2Seq framework is robust to this distributional shift, outperforming almost all baselines. This is particularly evident in the performance of Set2Seq Transformer variants, which maintain strong results across most ranking criteria despite the temporal shift. We also observe that methods explicitly modeling temporal structure, such as LSTM, Transformer,

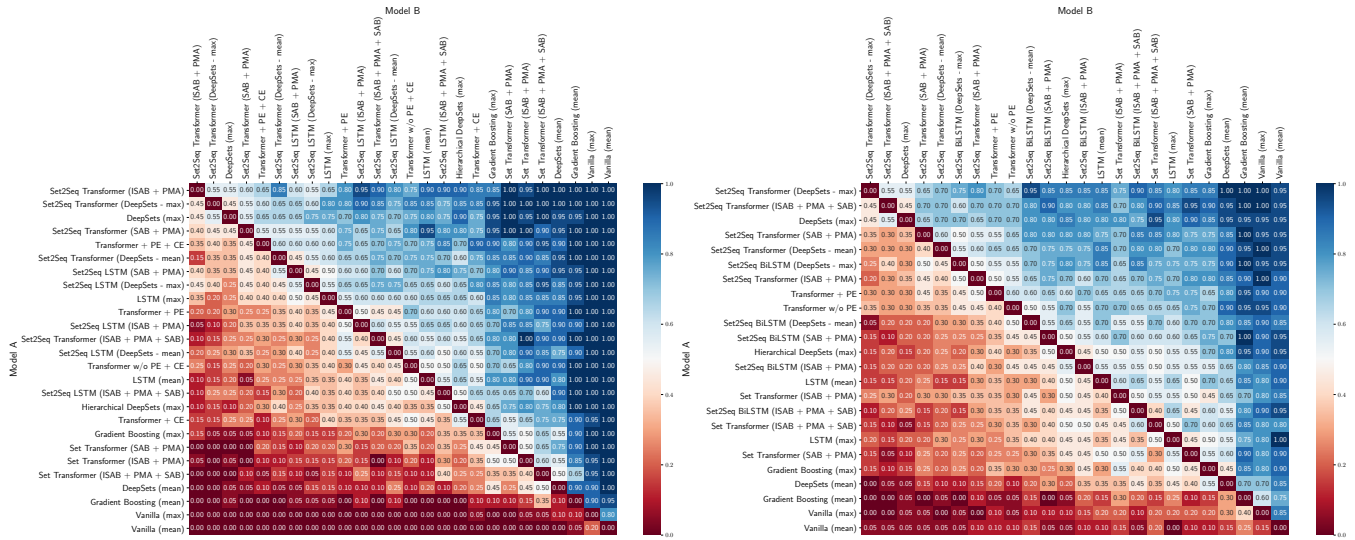


Figure 5: Pairwise win-rate heatmap showing the fraction of times Model A (rows) defeats Model B (columns) in pairwise comparisons for the Stratified Split (left) and Time Series Split (right). Models are ordered by their average win-rate across all comparisons.

and Set2Seq, show greater resilience than static baselines in this challenging setting.

Leaderboard and aggregate performance. To summarize overall performance across artist ranking criteria, we report two aggregate leaderboard scores: the Bradley–Terry (BT) score and a Borda count–based score, following the evaluation protocol described in Section 4.1 of the main paper. BT scores are derived from pairwise win–loss comparisons between methods across all metric evaluations, using the Bradley–Terry model [14] as detailed in [25]. Borda scores [27] are obtained by ranking methods per metric and dataset, then summing rank-based points to produce a global ordering. Under the Time Series Split, Set2Seq Transformer variants achieve the highest scores across both leaderboards and aggregate metrics. The Set2Seq Transformer with DeepSets and max pooling as the set-based module achieves the best Borda score and ranks second in BT score, while the Set2Seq Transformer with Set Transformer (ISAB + PMA + SAB) achieves the highest Kendall’s τ and ties for the lowest MAE. Interestingly, DeepSets with max pooling also performs exceptionally well, achieving the highest BT score and a Borda score comparable to top Set2Seq variants—reinforcing our earlier observations about the expressive capacity of large static sets.

Pairwise model comparison using win-rate heatmaps. Figure 5 presents pairwise win-rate heatmaps for all models evaluated on the WikiArt-Seq2Rank dataset under both the Stratified and Time Series splits. Each cell shows the fraction of times Model A (row) outperforms Model B (column) across all ranking criteria. We follow the methodology introduced in [25], where pairwise win rates are used to visualize head-to-head comparisons in a structured, interpretable manner. Models are ordered by their average win rate across pairwise comparisons. Variants of the Set2Seq Transformer consistently achieve top rankings. Notably, the Set2Seq Transformer variant using DeepSets with max pooling achieves the highest average win rate in the Time Series split and ranks second overall in the Stratified split, highlighting its robustness under both standard and

temporally shifted evaluation settings. Across both splits, Set2Seq variants dominate the top positions, with only two baseline methods—DeepSets with max pooling and the Transformer with both positional encoding and temporal embeddings—ranking comparably. These results further highlight the effectiveness of combining set-based and temporal modeling in the Set2Seq framework.

Results using alternative visual backbones. In our main experiments, we utilize a frozen ResNet-34 [52] backbone pre-trained on ImageNet [31] to extract feature vectors representing each visual instance x_i described in Eq. (2) of the main paper. While this setup provides strong baseline representations, it does not account for domain specificity or recent advances in multimodal pretraining. To explore this further, we evaluate a diverse set of alternative visual backbones, including multimodal models, standard unimodal vision architectures, and models fine-tuned on art-specific tasks.

Multimodal methods. We employ the following three multimodal methods to extract visual feature vectors, each leveraging pretrained vision–language representations and widely used in cross-modal learning tasks:

- Clip. We utilize a Clip [96] variant using a ViT-B-16 module.
- Blip. We utilize Blip [74] based on the LLanguage-VISion (Lavis) library implementation [72].
- Blip2. We utilize Blip2 [73] based on the LLanguage-VISion (Lavis) library implementation [72].

Unimodal methods. We employ the following four different vision unimodal methods pre-trained on ImageNet to extract visual feature vectors:

- VGG. We utilize a VGG-19 variant [103].
- ResNet. We utilize ResNet-18, ResNet-34, ResNet-50, ResNet-101 and ResNet-152 backbones [52].
- ConvNeXt. We utilize a ConvNeXt base architecture [80].
- ViT. We utilize a ViT-B-16 variant [36].

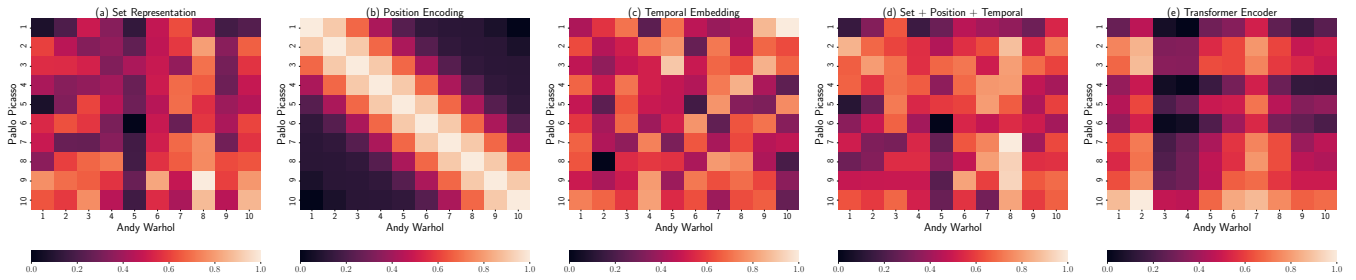


Figure 6: Visualization of pairwise cosine distances between the first ten years of the top-2 ranked artists’ careers based on the Aggregate Ranking (Pablo Picasso and Andy Warhol). (a) illustrates the pairwise cosine distance between the set representations of the first ten years of Pablo Picasso and Andy Warhol’s careers. (b) illustrates the Position Encoding. (c) illustrates the Temporal Embeddings. (d) illustrates the aggregate of the set representations, positional encodings and temporal embeddings. (e) illustrates the final output obtained from the Transformer module. Lighter denotes higher cosine similarity.

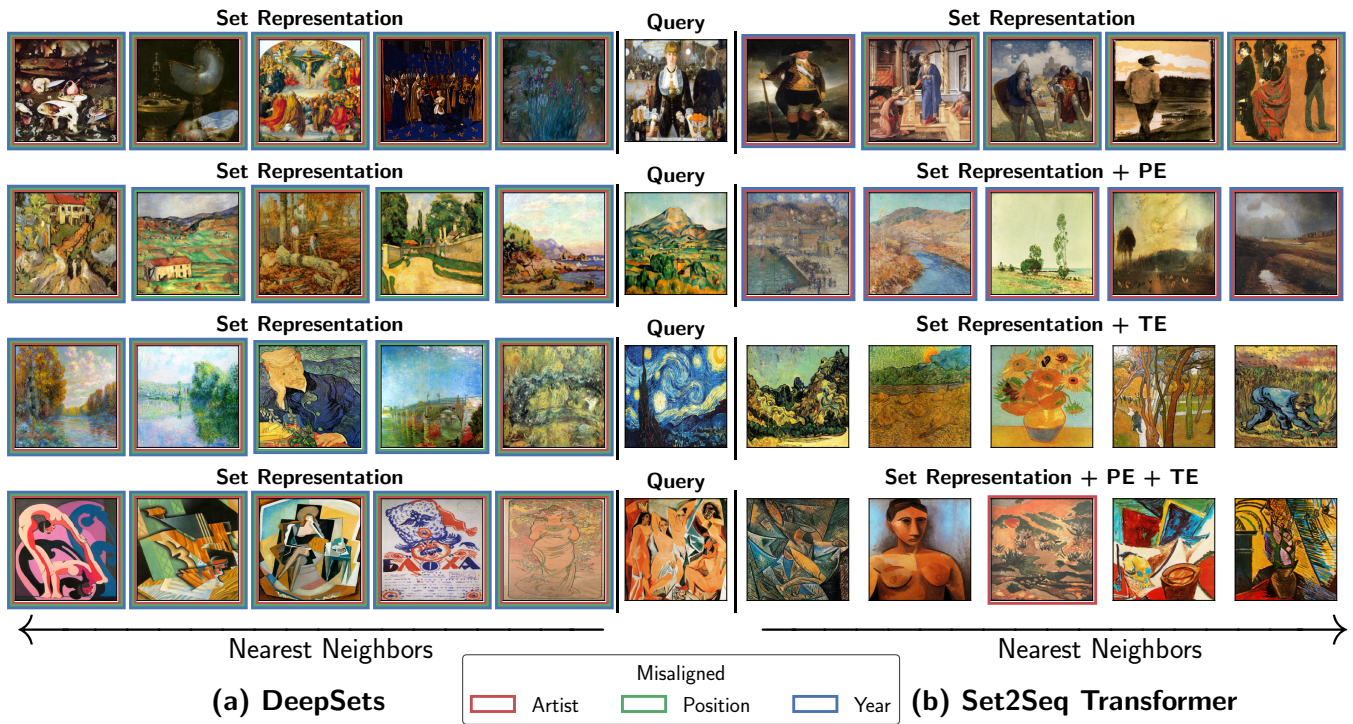


Figure 7: Qualitative analysis of learned visual representations for single-instance painting retrieval. Given a reference painting (middle), the top-5 nearest neighbors of DeepSets (left) and Set2Seq Transformer were retrieved (right). Misaligned patches denote paintings attributed with different **artist**, **position** or **year** annotation(s) from the reference painting.

Art-specific fine-tuned architectures. We employ three different methods pre-trained for art-specific tasks to extract visual feature vectors:

- ResNet-152 (Tag Prediction). We utilize a ResNet-152 architecture fine-tuned for the WikiArt tag prediction task [39].
- ArtSAGENet (Tag Prediction). We utilize the ArtSAGENet architecture fine-tuned for the WikiArt tag prediction task [39].
- ArtSAGENet (MTL). We utilize the multi-task learning (MTL) ArtSAGENet architecture fine-tuned for the WikiArt style

classification, artist attribution, and creation period estimation tasks [39].

Tables 7 and 8 report the results using different visual feature extractors using the Gradient Boosting baseline as described in Section B. It can be clearly seen that utilizing methods fine-tuned for art-specific tasks can improve performance compared to frozen pre-trained on ImageNet methods. Another observation is that employing multimodal methods for visual feature extraction also helps

Table 7: Results for the predicting artistic success task using the WikiArt-Seq2Rank Stratified Split validation set with Gradient Boosting and max aggregation. We report Kendall’s τ and Mean Absolute Error (MAE) for different visual feature extractors and rankings. For Kendall’s τ higher (Δ) is better. For MAE lower (∇) is better. Best results in bold; second best underlined.

Method	eBooks		The New York Times		Wikipedia Mentions		Wikipedia Links		Wikipedia Pageviews		Google Ngram		Google Trends		Artfacts		Artprice		Aggregate Ranking		Average	
	τ Δ	MAE ∇	τ Δ	MAE ∇	τ Δ	MAE ∇	τ Δ	MAE ∇	τ Δ	MAE ∇	τ Δ	MAE ∇	τ Δ	MAE ∇	τ Δ	MAE ∇	τ Δ	MAE ∇	τ Δ	MAE ∇	τ Δ	MAE ∇
CLIP	0.319	<u>0.170</u>	0.179	0.111	0.291	0.092	0.251	0.088	0.385	<u>0.202</u>	0.272	0.252	0.258	0.205	0.480	0.198	0.323	0.203	0.261	<u>0.208</u>	0.302	<u>0.173</u>
BLIP	0.350	0.172	0.355	0.115	0.300	0.100	0.330	0.091	0.292	0.236	0.361	0.228	0.219	0.212	0.433	0.215	0.256	0.223	0.322	0.217	0.322	0.181
BLIP2	0.331	0.185	0.247	<u>0.117</u>	0.336	0.083	0.216	0.101	0.307	0.230	0.128	0.269	0.198	0.211	0.380	0.229	0.271	0.210	0.289	0.220	0.270	0.186
VGG-19	0.144	0.230	0.305	0.097	0.184	0.104	0.200	0.098	0.331	0.225	0.271	0.257	0.315	0.191	0.424	0.225	0.321	0.185	0.183	0.237	0.268	0.185
ResNet-18	0.208	0.215	0.300	0.112	0.108	0.101	0.293	0.081	0.302	0.228	0.226	0.270	0.213	0.213	0.405	0.215	0.318	0.195	0.282	0.218	0.265	0.185
ResNet-34	0.267	0.196	0.312	<u>0.107</u>	0.202	0.092	0.232	0.088	0.348	0.209	0.191	0.272	0.252	0.204	0.356	0.239	0.238	0.211	0.244	0.223	0.264	0.184
ResNet-50	0.341	0.206	0.210	0.129	0.201	0.108	0.319	0.093	0.363	0.210	0.246	0.251	0.221	0.215	0.412	0.220	0.272	0.218	0.293	0.210	0.288	0.186
ResNet-101	<u>0.366</u>	0.185	0.203	0.137	0.281	0.088	0.209	0.092	0.346	0.209	0.258	0.244	0.241	0.210	0.422	0.228	0.244	0.234	0.187	0.250	0.276	0.188
ResNet-152	0.280	0.206	0.278	0.115	0.236	0.097	0.313	<u>0.085</u>	<u>0.376</u>	0.204	0.233	0.270	0.191	0.224	0.380	0.219	<u>0.338</u>	<u>0.186</u>	0.228	0.229	0.285	0.184
ConvNeXt	0.279	0.208	0.334	0.110	0.245	0.090	0.330	0.090	0.282	0.243	0.174	0.275	0.143	0.227	0.412	0.225	0.123	0.237	0.259	0.223	0.248	0.193
ViT	0.267	0.205	0.301	0.111	0.248	0.092	0.302	0.086	0.254	0.231	0.234	0.261	0.285	0.194	0.350	0.235	0.325	0.201	<u>0.347</u>	0.209	0.291	0.183
ResNet-152 (Tag Prediction)	0.323	0.190	0.340	0.112	0.198	0.109	0.373	0.090	0.285	0.225	0.126	0.276	0.286	0.207	0.407	0.223	0.241	0.212	0.244	0.232	0.282	0.188
ArtSAGENet (Tag Prediction)	0.327	0.179	0.289	0.109	<u>0.313</u>	0.089	0.232	0.091	0.340	0.215	0.278	0.252	<u>0.337</u>	0.211	0.275	0.250	0.186	0.221	0.336	0.209	0.291	0.183
ArtSAGENet (MTL)	0.492	0.138	<u>0.342</u>	<u>0.107</u>	0.204	<u>0.085</u>	<u>0.342</u>	0.090	0.364	0.196	<u>0.343</u>	<u>0.232</u>	0.375	0.180	0.438	<u>0.205</u>	0.347	0.197	0.486	0.176	0.373	0.161

Table 8: Results for the predicting artistic success task using the WikiArt-Seq2Rank Time Series Split validation set with Gradient Boosting and max aggregation. We report Kendall’s τ and Mean Absolute Error (MAE) for different visual feature extractors and rankings. For Kendall’s τ higher (Δ) is better. For MAE lower (∇) is better. Best results in bold; second best underlined.

Method	eBooks		The New York Times		Wikipedia Mentions		Wikipedia Links		Wikipedia Pageviews		Google Ngram		Google Trends		Artfacts		Artprice		Aggregate Ranking		Average	
	τ Δ	MAE ∇	τ Δ	MAE ∇	τ Δ	MAE ∇	τ Δ	MAE ∇	τ Δ	MAE ∇	τ Δ	MAE ∇	τ Δ	MAE ∇	τ Δ	MAE ∇	τ Δ	MAE ∇	τ Δ	MAE ∇	τ Δ	MAE ∇
CLIP	0.304	0.197	0.205	0.176	0.260	0.110	0.193	0.133	0.188	0.248	0.042	0.257	0.045	0.244	0.250	0.244	0.175	0.284	0.272	0.235	0.193	0.213
BLIP	0.228	0.211	0.270	0.167	0.262	0.122	0.283	0.130	0.213	0.237	0.134	<u>0.237</u>	0.093	0.221	0.361	0.218	0.060	0.318	<u>0.366</u>	<u>0.208</u>	0.227	0.207
BLIP2	0.300	0.225	0.284	0.167	0.298	0.109	0.311	0.129	0.124	0.257	0.111	0.246	0.032	<u>0.203</u>	<u>0.323</u>	<u>0.234</u>	0.177	0.289	0.268	0.217	0.223	0.208
VGG-19	0.253	0.183	0.166	0.159	0.152	0.120	0.235	0.125	0.193	0.239	0.140	0.248	0.110	0.223	0.176	0.265	0.163	0.272	0.276	0.231	0.186	0.206
ResNet-18	0.281	0.201	0.296	<u>0.137</u>	0.306	<u>0.100</u>	0.275	0.115	0.086	0.253	-0.004	0.263	0.072	0.222	0.176	0.261	0.154	<u>0.266</u>	0.236	0.226	0.188	<u>0.204</u>
ResNet-34	0.246	0.228	0.303	0.152	0.218	0.117	0.189	0.128	0.166	0.260	0.004	0.252	0.144	0.224	0.221	0.250	0.132	0.301	0.176	0.246	0.180	0.216
ResNet-50	0.295	0.199	0.287	0.158	0.238	0.120	<u>0.335</u>	0.121	0.247	0.218	0.105	0.245	0.145	0.222	0.224	0.253	0.130	0.303	0.123	0.252	0.213	0.209
ResNet-101	0.106	0.212	0.209	0.160	0.177	0.115	0.195	0.124	0.195	0.235	-0.059	0.276	0.130	0.229	0.090	0.284	0.163	0.293	0.235	0.241	0.144	0.217
ResNet-152	0.184	0.220	0.282	0.160	0.334	0.123	0.313	0.134	0.207	0.247	0.068	0.249	0.040	0.247	0.142	0.276	0.232	0.279	0.205	0.233	0.201	0.217
ConvNeXt	0.266	0.195	0.162	0.170	0.188	0.120	0.158	0.139	<u>0.282</u>	<u>0.229</u>	0.113	0.239	0.162	0.205	0.251	0.242	0.244	0.280	0.248	0.220	0.207	<u>0.204</u>
ViT	<u>0.345</u>	0.192	0.283	0.136	0.413	0.095	0.261	<u>0.119</u>	0.141	0.247	0.115	0.242	<u>0.226</u>	0.212	0.194	0.258	0.209	0.280	0.350	0.212	<u>0.254</u>	0.199
ResNet-152 (Tag Prediction)	0.311	<u>0.188</u>	<u>0.308</u>	0.157	0.299	0.125	0.252	0.155	0.130	0.257	0.008	0.257	0.079	0.223	0.114	0.275	0.298	0.247	0.198	0.241	0.200	0.212
ArtSAGENet (Tag Prediction)	0.172	0.195	0.220	0.182	0.262	0.116	0.161	0.152	0.220	0.241	<u>0.185</u>	0.238	0.253	0.194	0.231	0.258	0.075	0.316	0.269	0.230	0.205	0.212
ArtSAGENet (MTL)	0.357	0.231	0.404	0.185	<u>0.369</u>	0.119	0.423	0.123	0.337	0.232	0.322	0.216	0.139	0.228	0.268	0.242	<u>0.266</u>	0.270	0.393	0.197	0.328	<u>0.204</u>

improve performance over unimodal methods pre-trained on ImageNet, especially in the case of the Stratified Split setting. In contrast, evaluation on the Time Series Split setting shows that unimodal methods can perform comparably to the multimodal counterparts. Note that for simplicity and fair comparison among the different static and temporal-aware multiple-instance learning methods, in this work we utilize a ResNet-34 backbone as a visual feature extractor for all methods considered.

D Mesogeos Dataset

This section presents the variables used for the Mesogeos short-term wildfire danger forecasting task, details of the extended temporal embedding implementation, and ablation studies for the Set2Seq Transformer variants.

D.1 Wildfire Danger Forecasting Variables

Table 9 summarizes the numerical variables for the short-term wildfire danger forecasting task, selected to capture key wildfire drivers [66]. To ensure a fair comparison of methods, we strictly adhere to the preprocessing and variable definitions outlined in [66]. The target variable is a binary indicator of wildfire danger, derived from the feature burned_area_has, which represents the burned area in hectares within a designated buffer zone. That is, if the burned area

exceeds 30 hectares, the wildfire danger variable is set to 1; otherwise, it is set to 0.

Meteorological variables, such as Max Temperature (t2m), Min Relative Humidity (rh), and Total Precipitation (tp), are sourced from ERA5-Land [91]. Vegetation and land surface properties, including Normalized Difference Vegetation Index (ndvi), Leaf Area Index (lai), and Land Surface Temperatures (lst_day and lst_night), are obtained from MODIS [34, 92, 121].

Other environmental features include the Soil Moisture Index (smi) derived from the European Drought Observatory (EDO) [16], and land cover fractions, such as fractions of agriculture (lc_agriculture) and forest (lc_forest), sourced from Copernicus Climate Change Services (CCS) products [28]. Human-related variables include population density (population) and roads distance (roads_distance), obtained from WorldPop [113]. Elevation data (dem) and its derivatives, such as slope, are provided by COP-DEM [41].

To capture temporal dynamics, we employ a temporal embedding based on the full timestamp information available in the Mesogeos dataset. This approach extends the simpler temporal embedding used in the WikiArt-Seq2Rank task, where only the creation year is available for each artwork. By utilizing the full timestamp, the embedding in this context captures finer-grained temporal patterns, which are critical for accurately forecasting wildfire danger.

Table 9: Numerical variables for the short-term wildfire danger forecasting using the Mesogeos [66]. The values in the column ‘Feature Name’ correspond to the variable names used in the dataset.

Variable	Spatial	Temporal	Units	Type	Feature Name
Max Temperature	9 km	Hourly	K	Dynamic	t2m
Max Dewpoint Temperature	9 km	Hourly	K	Dynamic	d2m
Max Wind Speed	9 km	Hourly	m/s	Dynamic	wind_speed
Max Surface Pressure	9 km	Hourly	Pa	Dynamic	sp
Min Relative Humidity	9 km	Hourly	%/100	Dynamic	rh
Total Precipitation	9 km	Hourly	m	Dynamic	tp
Mean Surface Solar Radiation Downwards	9 km	Hourly	J/m ²	Dynamic	ssrd
Day Land Surface Temperature	1 km	Daily	K	Dynamic	lst_day
Night Land Surface Temperature	1 km	Daily	K	Dynamic	lst_night
Normalized Difference Vegetation Index (NDVI)	500 m	16-days	-	Dynamic	ndvi
Leaf Area Index (LAI)	500 m	8-days	-	Dynamic	lai
Soil moisture	5 km	10-days	-	Dynamic	smi
Timestamp	-	Daily	Datetime	Dynamic	time
Population	1 km	Yearly	people/km ²	Semi-Static	population
Fraction of agriculture	300 m	Yearly	%/100	Semi-Static	lc_agriculture
Fraction of forest	300 m	Yearly	%/100	Semi-Static	lc_forest
Fraction of grassland	300 m	Yearly	%/100	Semi-Static	lc_grassland
Fraction of settlements	300 m	Yearly	%/100	Semi-Static	lc_settlement
Fraction of shrubland	300 m	Yearly	%/100	Semi-Static	lc_shrubland
Fraction of sparse vegetation	300 m	Yearly	%/100	Semi-Static	lc_sparse_vegetation
Fraction of water bodies	300 m	Yearly	%/100	Semi-Static	lc_water_bodies
Fraction of wetland	300 m	Yearly	%/100	Semi-Static	lc_wetland
Roads distance	1 km	Static	km	Static	roads_distance
Elevation	30 m	Static	m	Static	dem
Slope	30 m	Static	rad	Static	slope
Wildfire Danger	1 km	Daily	Binary (0/1)	Target	burned_area_has

D.2 Temporal Embedding

To effectively capture temporal dynamics in wildfire danger forecasting, we extend the temporal embedding approach from the WikiArt-Seq2Rank task. While WikiArt used only creation years, the Mesogeos dataset provides full timestamps, enabling more flexible embeddings with day, month, and year components. In this work, we focus on month-year embeddings for their balance of granularity and noise reduction.

The temporal embedding $\mathbf{v}_i \in \mathbb{R}^H$ for a timestep $t_i = (m, a)$, where m denotes the month and a denotes the year, is computed as:

$$\mathbf{v}_i = [\mathbf{v}_i^m, \mathbf{v}_i^a], \quad (18)$$

where $\mathbf{v}_i^m \in \mathbb{R}^{H/2}$ encodes the month m and $\mathbf{v}_i^a \in \mathbb{R}^{H/2}$ encodes the year a . The concatenation produces the final temporal embedding of size H .

Month encoding (\mathbf{v}_i^m). Our cyclic encoding for months is inspired by the Time2Vec framework [63], which uses learnable sine and cosine functions to represent periodic temporal patterns. We employ learnable frequency and phase parameters to adaptively encode cyclic patterns. The month encoding uses sine and cosine functions with learnable parameters for frequency (ω_m) and phase (ϕ_m):

$$\mathbf{v}_i^m = [\sin(\omega_m m + \phi_m), \cos(\omega_m m + \phi_m)], \quad (19)$$

Here, m represents the normalized month, computed as:

$$m = \frac{\text{month}}{12} \cdot 2\pi, \quad (20)$$

where $\text{month} \in 1, 2, \dots, 12$, $\omega_m \in \mathbb{R}^{H/4}$ is a learnable frequency vector, and $\phi_m \in \mathbb{R}^{H/4}$ is a learnable phase vector. The final month embedding, combining sine and cosine components, is of size $H/2$. **Year encoding (\mathbf{v}_i^a).** Unlike Time2Vec [63], which uses a simple linear term to encode temporal progression, our year embedding employs a feed-forward network (FFN) to capture complex, non-linear trends in temporal data. This flexibility is crucial for wildfire forecasting, where temporal patterns often involve abrupt shifts and non-linear trends due to climate and human activity. The year embedding is calculated using a feed-forward network $FFN(\cdot)$ combined with learnable weights and biases:

$$\mathbf{v}_i^a = FFN(a)\mathbf{w}_a + \mathbf{b}_a, \quad (21)$$

where a is the normalized year value, computed as:

Table 10: Results for the Mesogeos dataset using different Set Transformer modules for set representation learning. PE denotes utilizing positional encodings. CE denotes utilizing temporal embeddings. k denotes the number of instances for a set S at timestep t . l denotes the number of timesteps t for a sequence \mathcal{T} . For both metrics higher is better. Best results in bold; second best underlined.

Method	$k=1, l=30$		$k=2, l=15$		$k=3, l=10$		$k=5, l=6$		$k=10, l=3$	
	F1	PR-AUC								
Set2Seq Transformer (SAB + PMA) + PE	0.784	0.861	0.782	0.850	0.760	0.845	0.757	0.839	0.732	0.812
Set2Seq Transformer (SAB + PMA) + PE + CE	0.783	0.864	0.789	<u>0.862</u>	0.773	0.856	0.757	0.831	<u>0.751</u>	<u>0.823</u>
Set2Seq Transformer (ISAB + PMA) + PE	0.776	0.865	0.772	0.848	0.741	<u>0.851</u>	0.755	0.832	0.736	0.816
Set2Seq Transformer (ISAB + PMA) + PE + CE	0.784	0.866	<u>0.783</u>	0.861	<u>0.772</u>	0.856	0.771	0.850	0.761	0.835
Set2Seq Transformer (ISAB + PMA +SAB) + PE	<u>0.790</u>	<u>0.867</u>	0.773	0.852	0.770	0.844	<u>0.766</u>	0.835	0.747	0.809
Set2Seq Transformer (ISAB + PMA +SAB) + PE + CE	0.792	0.872	0.777	0.864	0.762	0.849	0.764	<u>0.840</u>	0.721	0.822

Table 11: Results for the Mesogeos dataset using different positional and temporal embeddings. PE denotes utilizing positional encodings. CE denotes utilizing temporal embeddings. (DM) denotes using the day and month, (MY) denotes using the month and year, and (DMY) denotes using the day, month and year as the timestamp feature. k denotes the number of instances for a set S at timestep t . l denotes the number of timesteps t for a sequence \mathcal{T} . For both metrics higher is better. Best results in bold; second best underlined.

Method	$k=1, l=30$		$k=2, l=15$		$k=3, l=10$		$k=5, l=6$		$k=10, l=3$	
	F1	PR-AUC								
Set2Seq Transformer (DeepSets)	0.703	0.786	0.717	0.772	0.712	0.786	0.721	0.785	0.738	0.796
Set2Seq Transformer (DeepSets) + PE	0.771	0.855	0.773	0.856	0.768	0.846	0.764	0.836	0.749	0.826
Set2Seq Transformer (DeepSets) + CE ^{MY}	0.737	0.812	0.734	0.812	0.767	0.822	0.746	0.814	0.737	0.813
Set2Seq Transformer (DeepSets) + PE + CE ^{DM}	0.782	0.859	<u>0.779</u>	0.856	<u>0.775</u>	<u>0.851</u>	0.772	0.844	0.763	0.831
Set2Seq Transformer (DeepSets) + PE + CE ^{MY}	0.784	0.864	0.761	0.863	0.768	0.833	0.756	0.830	0.747	<u>0.834</u>
Set2Seq Transformer (DeepSets) + PE + CE ^{DMY}	0.782	0.860	0.770	0.852	0.783	<u>0.851</u>	0.744	<u>0.849</u>	0.755	0.831
Set2Seq Transformer (ISAB + PMA)	0.755	0.853	0.756	0.850	0.748	0.837	0.769	0.834	0.727	0.797
Set2Seq Transformer (ISAB + PMA) + PE	0.776	0.865	0.772	0.848	0.741	<u>0.851</u>	0.755	0.832	0.736	0.816
Set2Seq Transformer (ISAB + PMA) + CE ^{MY}	0.786	0.871	0.777	0.845	0.734	0.811	0.753	0.835	0.748	0.822
Set2Seq Transformer (ISAB + PMA) + PE + CE ^{DM}	<u>0.791</u>	0.863	0.766	0.846	0.767	0.834	0.736	0.838	0.740	0.821
Set2Seq Transformer (ISAB + PMA) + PE + CE ^{MY}	0.784	<u>0.866</u>	0.783	<u>0.861</u>	0.772	0.856	<u>0.771</u>	0.850	<u>0.761</u>	0.835
Set2Seq Transformer (ISAB + PMA) + PE + CE ^{DMY}	0.796	0.864	0.783	0.854	0.773	0.850	0.745	0.839	0.754	0.827

$$a = \frac{\text{year} - \text{min_year}}{\text{max_year} - \text{min_year}}. \quad (22)$$

The feed-forward network $FFN(a)$ is defined as:

$$FFN(a) = \sigma(\mathbf{W}_1 \cdot a + \mathbf{b}_1) \mathbf{W}_2 + \mathbf{b}_2, \quad (23)$$

where σ is a non-linearity, such as the Rectified Linear Unit (ReLU), defined as:

$$\text{ReLU}(x) = \max(0, x). \quad (24)$$

Here, $\mathbf{W}_1, \mathbf{W}_2 \in \mathbb{R}^{H/4}$ are the weights of the feed-forward network, $\mathbf{b}_1, \mathbf{b}_2 \in \mathbb{R}^{H/4}$ are its biases, $\mathbf{w}_a \in \mathbb{R}^{H/2}$ is the learnable linear weight, and $\mathbf{b}_a \in \mathbb{R}^{H/2}$ is the learnable linear bias.

Final embedding. By combining cyclic and non-linear temporal representations, the final temporal embedding effectively captures both seasonal variations and long-term trends, enhancing the model performance for dynamic forecasting tasks. It is computed as the concatenation of the month and year embeddings, as shown in Eq. (18).

D.3 Additional Results

Here, we present additional results from evaluations of the Set2Seq Transformer, focusing on variations in its Set Transformer module configurations and temporal representations.

Set Transformer module configurations. Table 10 summarizes the performance of the Set2Seq Transformer with different Set Transformer modules for set representation learning. The results indicate that the Set Transformer (ISAB + PMA + SAB) configuration achieves superior performance on the short-term wildfire danger forecasting task in single-instance learning settings. Moreover, integrating temporal embeddings consistently improves performance over positional encoding-only variants. It is worth noting that the Set Transformer (ISAB + PMA) variant performs comparably to the other configurations in single-instance learning tasks, while outperforming them in multiple-instance learning scenarios.

Temporal representation strategies. Table 11 reports the results of ablation studies exploring alternative temporal position-aware representations for the Set2Seq Transformer. We experiment with different strategies for timestamp-based temporal embeddings integrated into set-based methods, such as Deep Sets and Set Transformer. The results demonstrate that incorporating temporal position-aware

representations significantly enhances performance compared to methods relying solely on positional encodings. The temporal embedding that utilizes month-year information derived from timestamps outperforms alternatives using day-month or day-month-year information, potentially due to its balance between granularity and reduced noise.

E Limitations and Broader Impact

This section discusses the methodological and dataset-specific challenges encountered in this work, highlighting directions for future improvement, and exploring the broader implications of our contributions across diverse domains.

E.1 Limitations

Rankings construction. The artist appreciation rankings in WikiArt-Seq2Rank provide a framework for analyzing artistic success by compiling data from diverse publicly available sources such as eBooks, Wikipedia, Artfacts, and Artprice, grounded in cultural industries theory [10, 100, 125]. These rankings are central to understanding artistic success as they capture multiple dimensions of recognition, including public interest, institutional acknowledgment, and commercial success, offering a unique perspective on the complex dynamics of cultural impact. However, as a proxy rather than an absolute measure, these rankings may reflect notoriety or controversy instead of positive recognition, and biases inherent in the source data—such as geographic, cultural, or institutional priorities—can influence the results. Therefore, while these rankings offer valuable insights, they should be interpreted cautiously and contextualized within the broader scope of artistic practices and historical influences to ensure meaningful conclusions.

Learning-to-Rank. In this work, we adopt a pointwise learning-to-rank approach by optimizing the Mean Squared Error (MSE) loss. This provides a simple and interpretable baseline for systematically comparing various methodologies. While MSE captures ranking trends, it does not directly optimize metrics such as Kendall’s τ or NDCG. Future work could explore pairwise and listwise approaches [17, 57], as well as other recent methods [134], to directly improve ranking performance.

Performance evaluation and benchmarking. In this paper, we benchmark the performance of various methods using the novel WikiArt-Seq2Rank dataset, and evaluate the generalization of our Set2Seq Transformer using the Mesogeos dataset. For fair evaluation, all methods were trained using the same hyperparameters, including batch size, optimizer, learning rate, and early stopping criteria, with minor adjustments for task-specific requirements. Our Set2Seq Transformer demonstrates robust performance, effectively learning temporal positional-aware set representations and consistently performing on par with or surpassing most baselines, showcasing strong generalization across tasks. While exhaustive hyperparameter optimization was beyond the scope of this work, task-specific tuning and advanced training strategies could further improve results. For instance, leveraging widely adopted techniques such as pre-training with masked inputs [33], autoregressive methods [15], and learning rate schedules (e.g., cosine warm-up [82]) could enhance the ability of Transformer-based methods to better capture temporal dependencies and improve training stability.

Complexity of learned temporal embeddings. The temporal embeddings in this work are designed to balance simplicity and expressiveness, adapting to the granularity of the datasets. For the WikiArt-Seq2Rank task, where only creation years are available, learnable year-based embeddings provide an effective and straightforward solution. For the Mesogeos dataset, a more advanced embedding leverages full timestamps to capture fine-grained temporal dynamics, which is critical for accurately modeling wildfire danger. Although the embedding approach for Mesogeos requires greater computational effort, it demonstrates substantial benefits in capturing temporal patterns and enhancing predictive performance. This dual framework underscores the adaptability of the temporal embeddings to diverse datasets and tasks, providing a foundation for future investigations into the trade-offs between complexity and efficiency.

E.2 Broader Impact

Interpretability in Transformer-based sequential multiple-instance learning. Our Set2Seq Transformer leverages attention mechanisms in both its Set Transformer module and Transformer layer, offering interpretability into the importance of individual set elements and the evolution of sequential temporal dependencies. For the WikiArt-Seq2Rank task, these mechanisms can uncover relationships between artists or artworks that drive rankings, revealing patterns of influence and recognition. Similarly, for the Mesogeos dataset, temporal attention can highlight critical periods or environmental factors influencing wildfire danger predictions. While this work does not explicitly explore these applications, the interpretability provided by attention weights and learned positional and temporal representations lays a solid foundation for future analyses in both artistic and environmental domains.

Applications to different domains. Modeling set-to-sequence relationships offers valuable opportunities for applications across creative domains such as literature, music, and film, where understanding temporal progression and patterns of creativity is essential. These methods could be used to analyze how authors, composers, or filmmakers evolve their craft over time, shedding light on artistic trajectories and innovation [29, 58, 85, 86, 116]. Furthermore, the positional and temporal embeddings developed in this work can be adapted to study broader phenomena in creativity and cultural influence, capturing an artist’s career stage or uncovering patterns shaped by historical and cultural contexts. By providing a flexible framework for integrating diverse types of input, these methods enable novel analyses and contribute to a deeper understanding of temporal and contextual dynamics in creative fields.

Effect of climate change. This work focuses on short-term wildfire danger forecasting using existing datasets and methodologies, without directly addressing the impact of climate change. However, the temporal embedding strategies introduced here, designed to capture fine-grained temporal dynamics, could be adapted to study long-term trends in wildfire patterns and their relationship to evolving climate conditions. Future research could build on these embeddings to analyze temporal trends in environmental variables, providing a framework for investigating connections between wildfire danger and climate change with appropriate validation and adaptation.